

Edge Localized Mode Control in DIII-D using Magnetic Perturbation-Induced Pedestal Transport Changes

R.A. Moyer¹

for

K.H. Burrell², T.E. Evans², M.E. Fenstermacher³, P. Gohil², I. Joseph¹, T.H. Osborne², M.J. Schaffer², P.B. Snyder², J.G. Watkins⁴, L.R. Baylor⁵, M. Bécoulet⁶, J.A. Boedo¹, N.H. Brooks², E.J. Doyle⁷, K.-H. Finken⁸, P. Garbet⁶, R.J. Groebner², M. Groth³, J. Harris⁵, E.M. Hollmann¹, G.L. Jackson², M. Jakubowski⁸, T.C. Jernigan⁵, S. Kasilov⁹, C.J. Lasnier³, A.W. Leonard², M. Lehnem⁸, J. Lönnroth¹⁰, E. Nardon⁶, V. Parail¹¹, G.D. Porter³, T.L. Rhodes⁷, D.L. Rudakov¹, A. Runov¹², O. Schmitz⁸, R. Schneider¹², D.M. Thomas², P. Thomas⁶, G. Wang⁷, W. P. West², L. Yan¹³, J.H. Yu¹, and L. Zeng⁷

1) University of California San Diego, La Jolla California

2) General Atomics, San Diego, California

3) Lawrence Livermore National Laboratory, Livermore California

4) Sandia National Laboratories, Albuquerque, New Mexico

5) Oak Ridge National Laboratory, Oak Ridge Tennessee

6) Association EURATOM-CEA, Cadarache France

7) University of California-Los Angeles, Los Angeles, CA

8) Forschungszentrum Jülich, Association EURATOM-FZJ, Jülich, Germany

9) Kharkov Institute for Physics and Technology, Kharkov, Ukraine

10) Association EURATOM-Tekes, Helsinki University of Technology, Finland

11) EURATOM-UKAEA Fusion Association, Culham Science Center, United Kingdom

12) Max Planck Institute for Physics, Greifswald, Germany

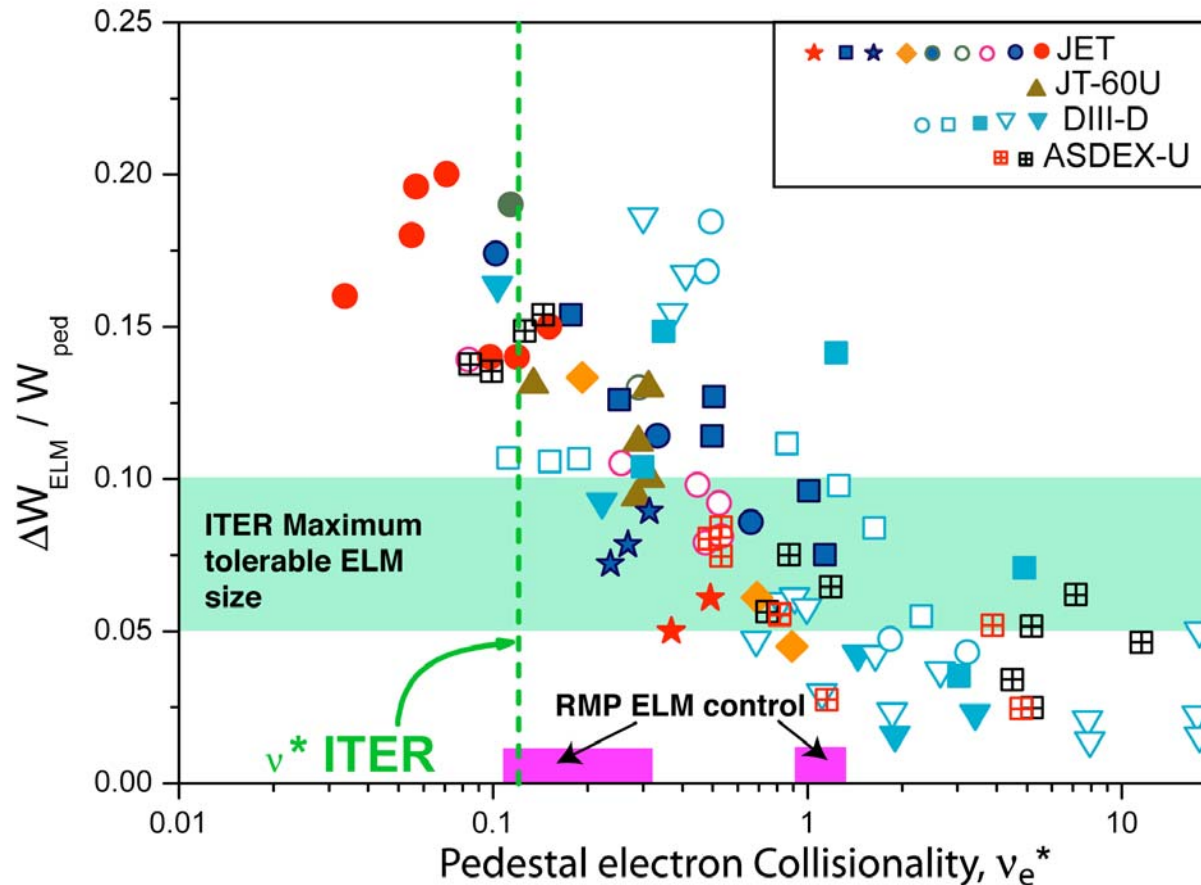
13) Southwest Institute for Physics, Chengdu, China

Presented at the
21st IAEA Fusion Energy Conference
Chengdu, China

October 16–21, 2006

ELM control is a critical issue for burning plasmas.

- $\Delta W_{\text{ELM}}/W_{\text{PED}}$ increases as pedestal collisionality ν_e^* drops



Loarte PPCF 45
1549

- Pedestal collisionality also affects RMP ELM control
 - RMP penetration decreases at lower ν_e^*
 - Parallel transport increases at lower ν_e^*

Summary and Results

- ELMs have been completely suppressed using an edge-resonant magnetic perturbation (RMP) in ELMy H-modes with ITER-relevant pedestal electron collisionality ν_e^* and ITER-similar shape (ISS).
- ELMs are suppressed by lowering the pedestal pressure gradient below the Peeling-Ballooning stability limit for Type I ELMs.
- Pedestal pressure gradient reduction is controlled with RMP strength $\delta b_r^{m,n}/B_T$.
- Pedestal pressure gradient is reduced primarily by increased particle transport
- Density fluctuations increase 1.5-2x during RMP, consistent with increased convective particle transport.

Edge Resonant Magnetic Perturbations (RMPs) suppress ELMs at ITER-relevant collisionalities in DIII-D

- Minimum perturbation $\delta b_r^{m,n}/B_T$ for ELM suppression varies with shape:

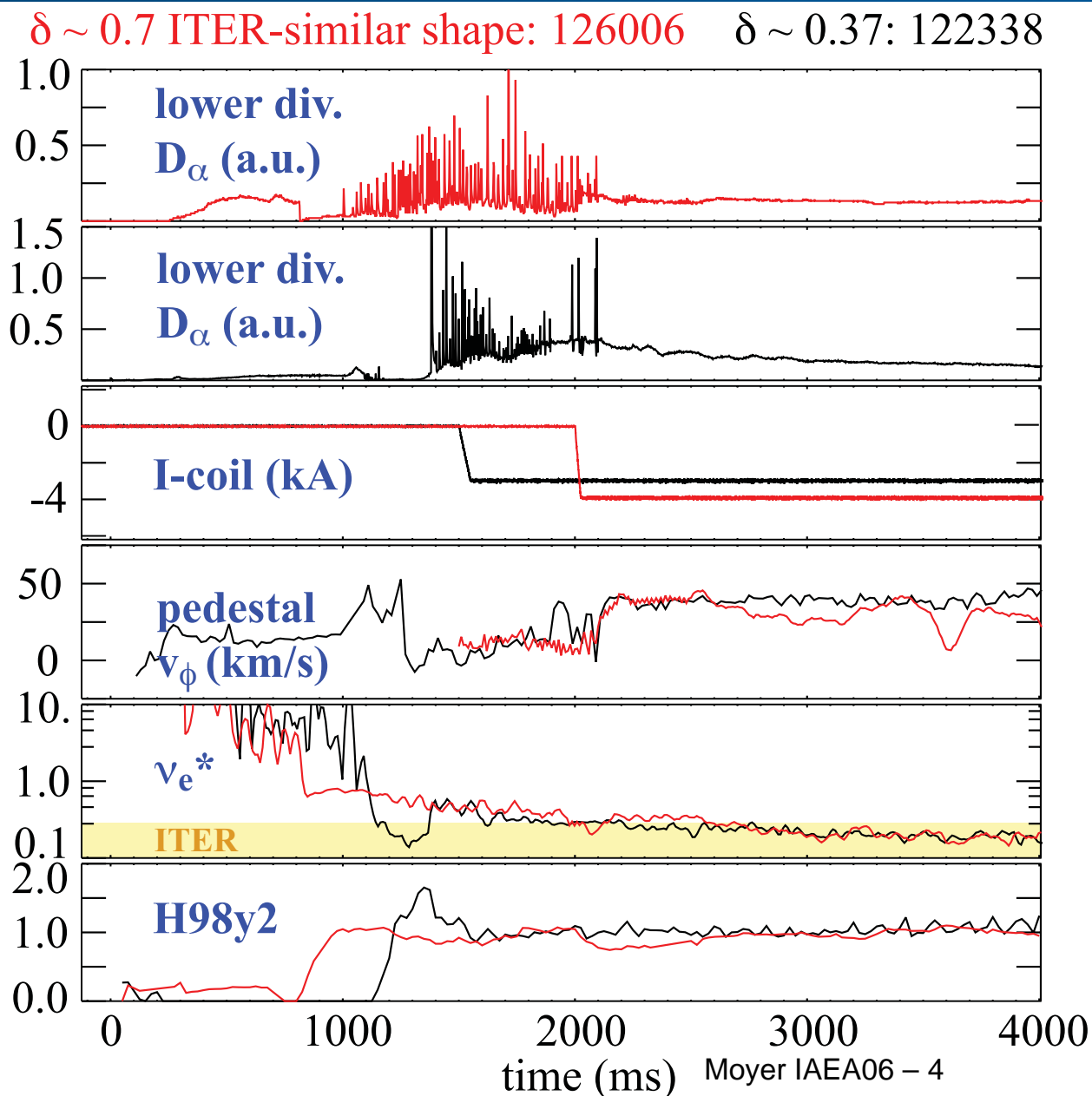
$$\delta b_r^{m,n}/B_T \sim 3.2 \times 10^{-4}$$

at $\delta \sim 0.7$

$$\delta b_r^{m,n}/B_T \sim 2.8 \times 10^{-4}$$

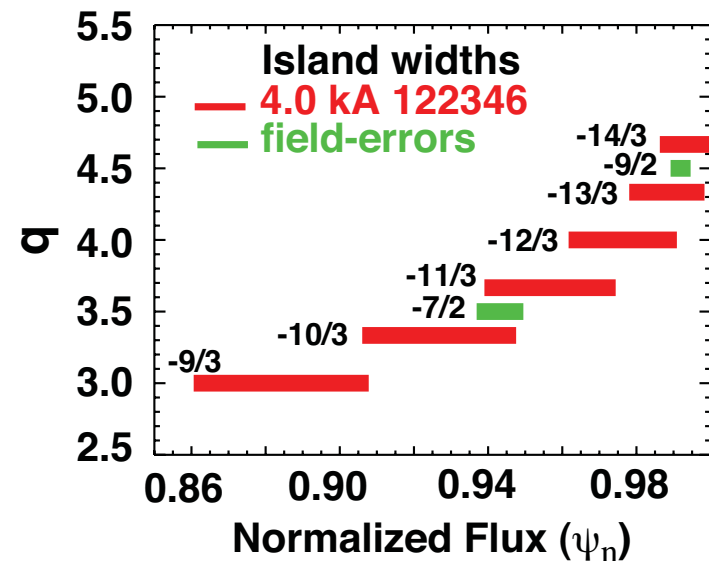
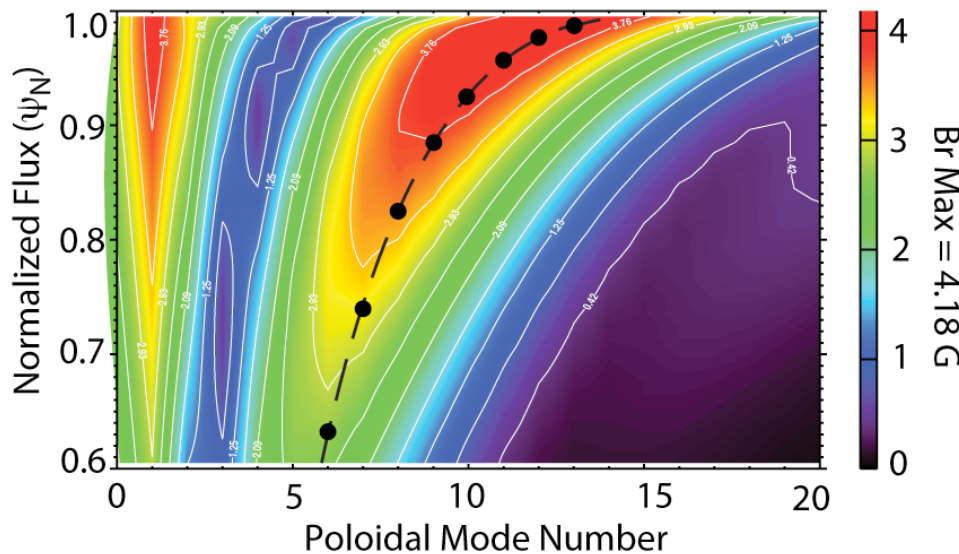
at $\delta \sim 0.37$

Burrell PPCF 47 B37 (05)
Evans Phys. Plasmas 13 (06)
Evans Nature Physics 2 419 (06)



Need to localize perturbation to pedestal to avoid degrading performance or triggering NTMs

- Elongation → slow pitch angle change with radius on LFS → low m 's not well localized by magnetic shear
- Magnetic shear → rational surfaces close together near separatrix → small RMP gives island overlap



- Magnetic field penetration model - [see V. Parail; M. Becoulet, this mtg.](#)
 - penetration high where collisionality is high and toroidal rotation is low → edge localized

$$B_{m,n}^{r,pl} = \frac{B_{m,n}^{r,vac}}{\sqrt{1 + (\Omega\tau_L/2m)^2}} \quad \text{where}$$

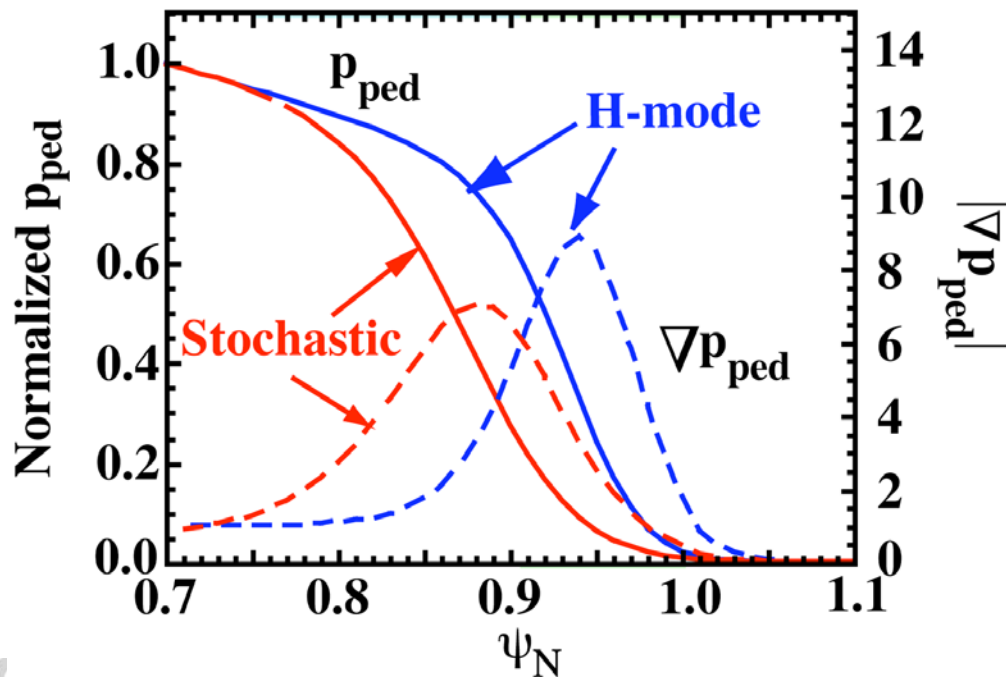
$$\Omega = 2\pi n f$$

$$\tau_L = 2 \left(\sqrt{1 + 2q^2 \tau_A} \right)^{2/3} \tau_\eta^{2/3} \tau_v^{-1/3}$$

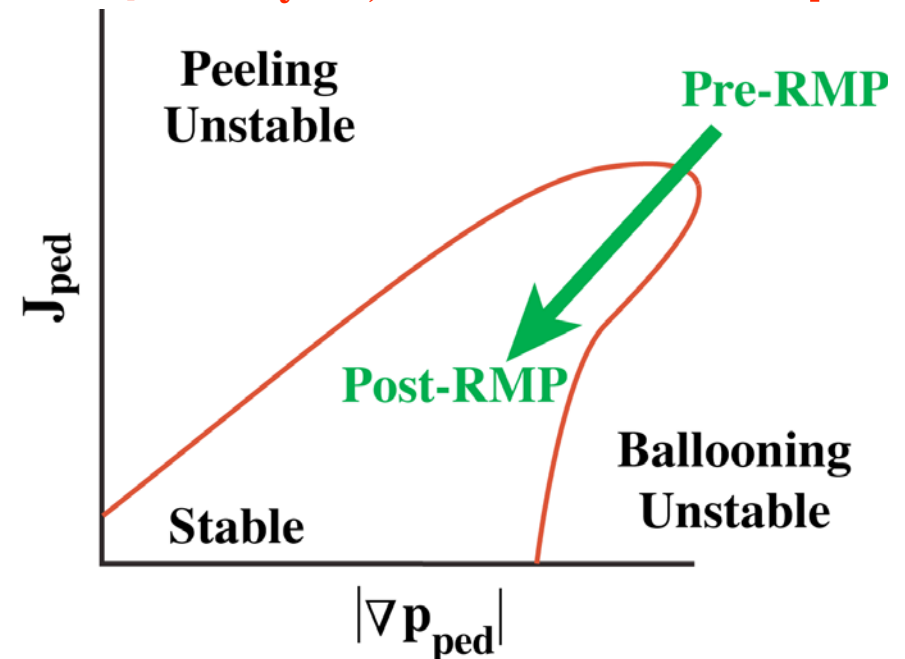
Use RMP to increase steady-state transport through pedestal to lower ∇p below ELM stability limit.

- Edge RMP \rightarrow stochastic field in pedestal \rightarrow increased steady-state transport
- Reduced ∇p_{ped} \rightarrow stable P-B operating point controlled by RMP amplitude
- Must maintain pedestal height (stiff core transport coupled to pedestal height).

Schematic Pedestal Profiles

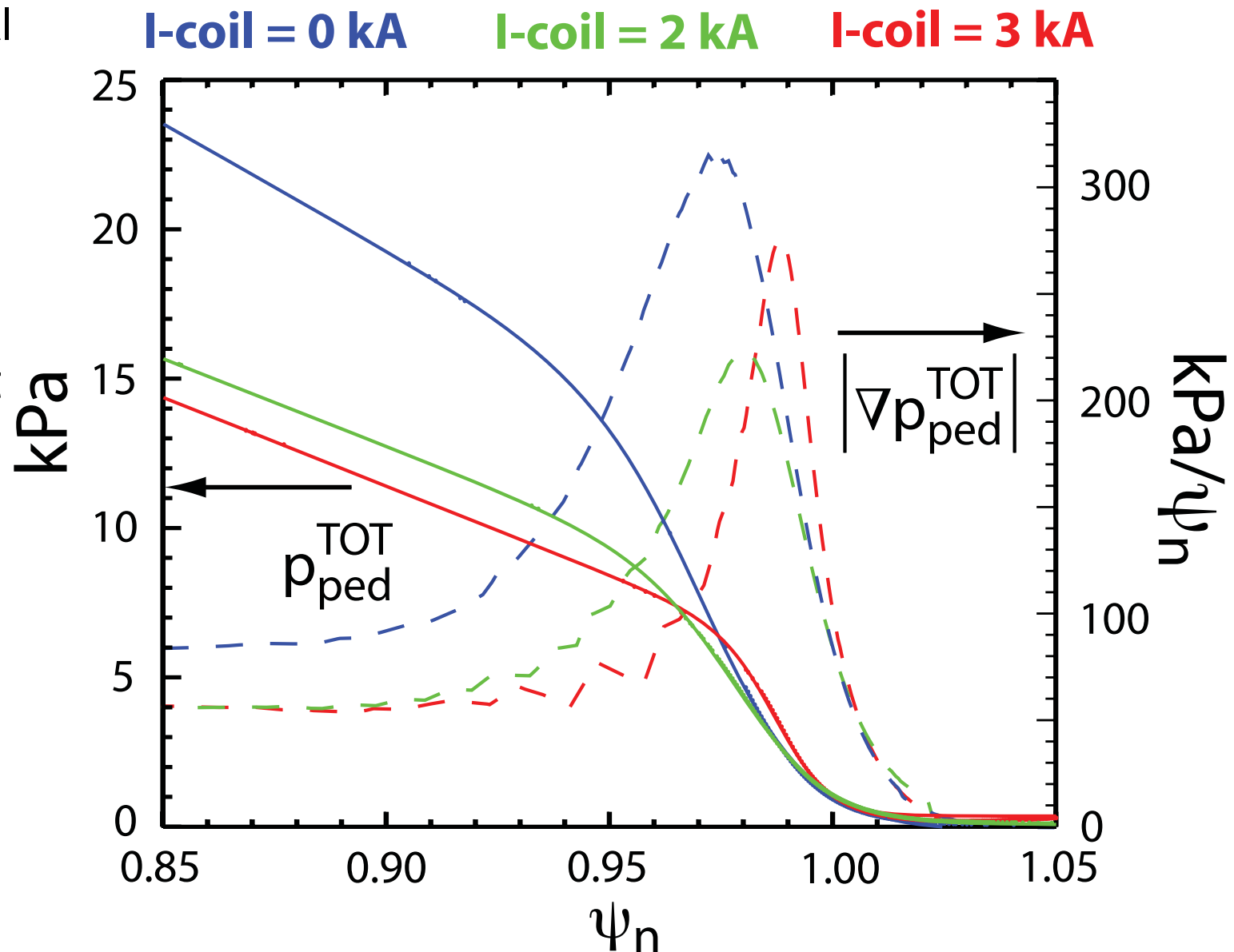


Schematic P-B Stability Diagram
[P.B. Snyder, H.R. Wilson PoP2002]



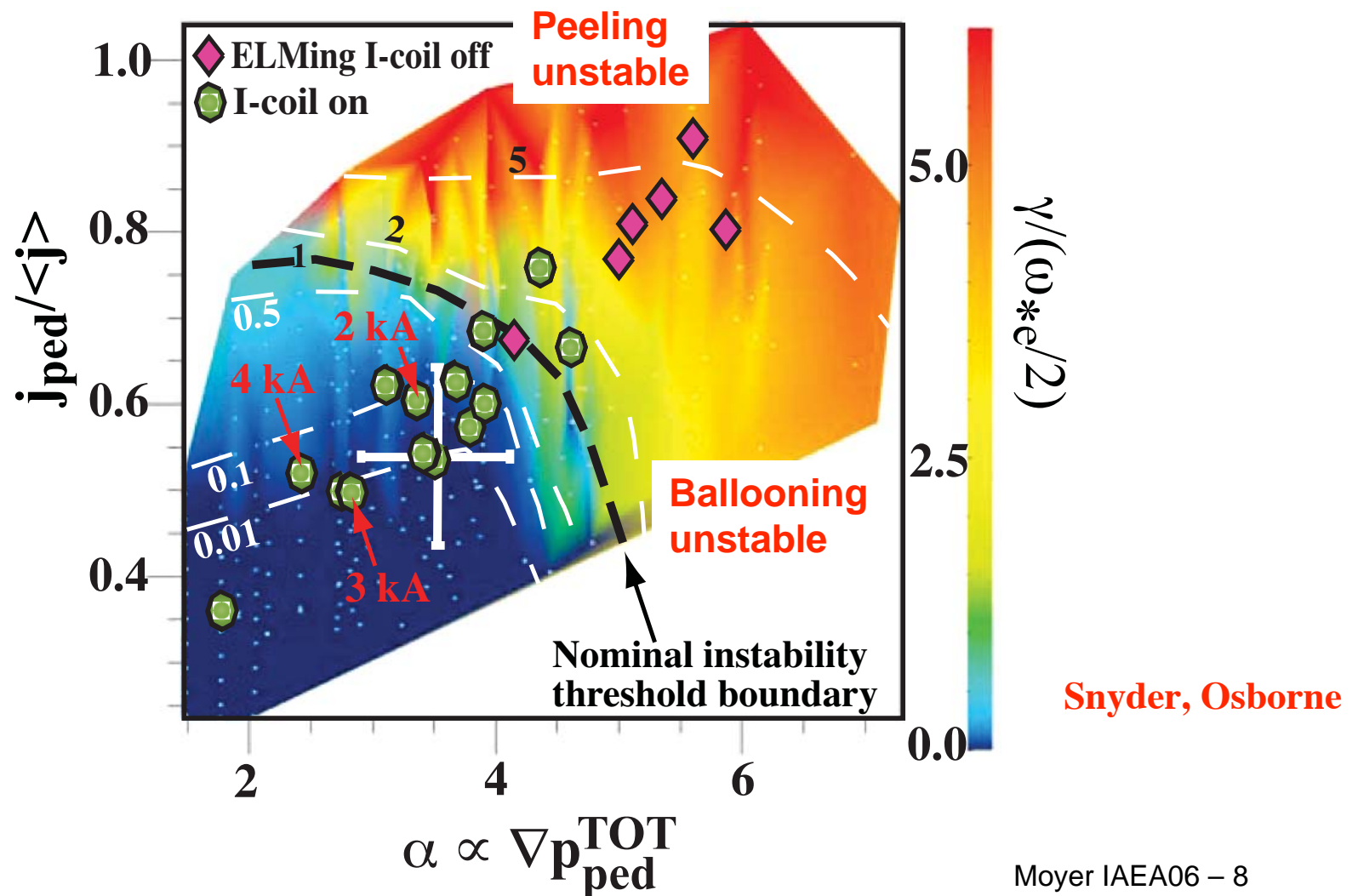
Edge RMP suppresses large ELMs by significantly lowering the pedestal pressure gradient.

- Total pedestal pressure is reduced during RMP pulse below P-B stability boundary
- I-coil current controls ∇p_{ped}
- ∇p_{ped} is reduced, narrowed, and shifted out in radius



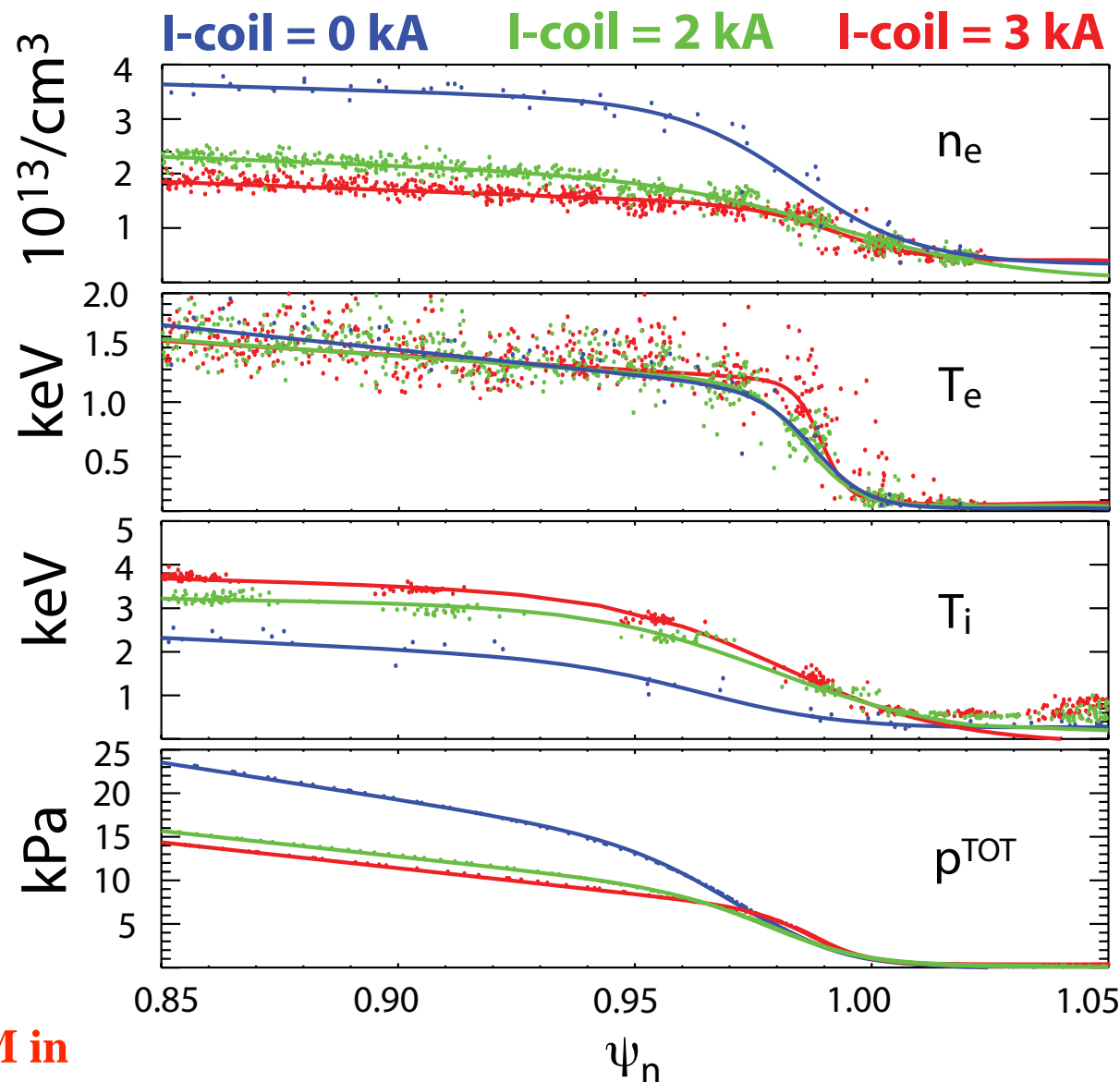
RMP-assisted ELM-free H-modes are linearly stable to Peeling-Ballooning modes.

- Increasing RMP can push pedestal deep into linearly stable regime; see P.B. Snyder, this meeting



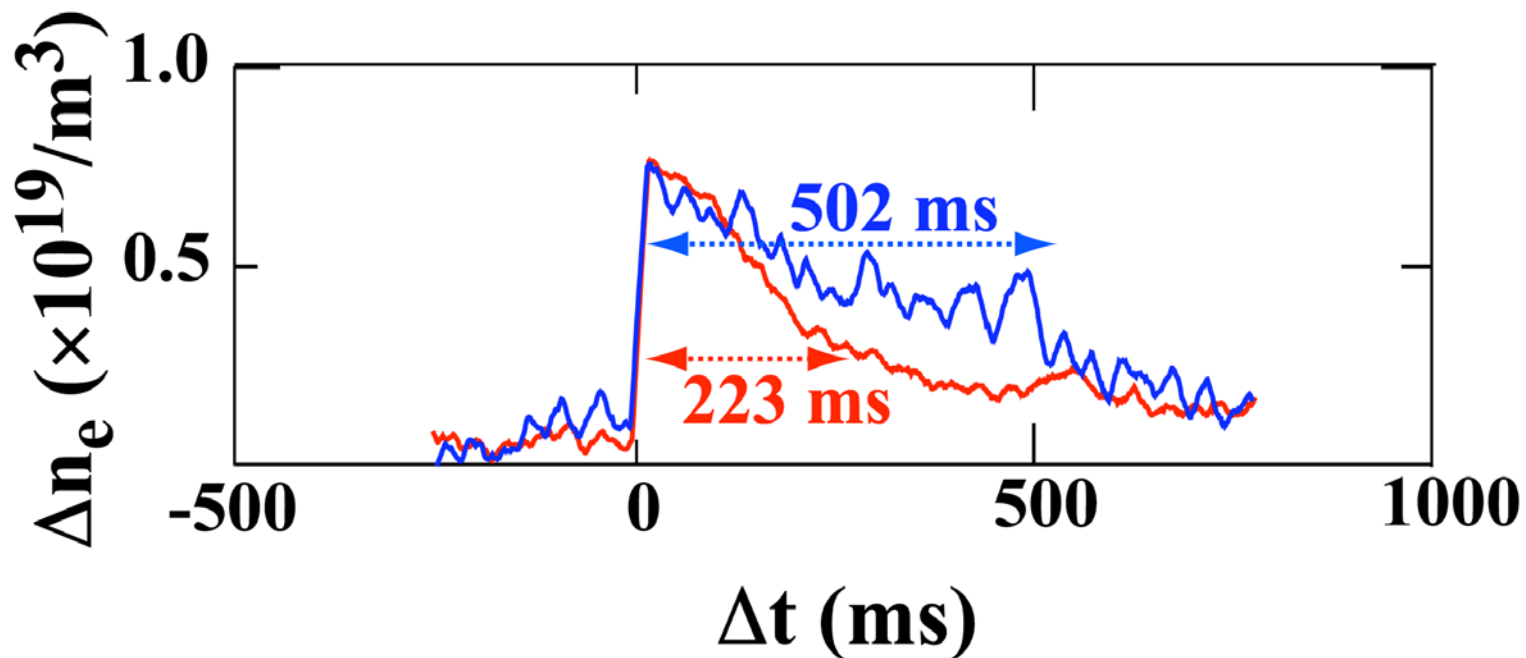
I-coil RMP has largest effect on density profile, not T_e profile at low collisionality.

- global particle balance change
 - P-B modes stabilized by density pumpout similar to QH mode [see P.B. Snyder this meeting]
 - QL estimate \rightarrow 3-4x increase in D_{eff}
- T_e profile flattens at top of pedestal
 - qualitatively consistent with quasi-linear estimate
 - quantitatively consistent for $0.85 < \psi_n < 0.94$ with transport analysis by Stacey and Evans
- T_e steepens for $0.98 < \psi_n < 1$
- Heat transport modeling with 3D fluid code E3D \rightarrow vac. field destroys H-mode pedestal



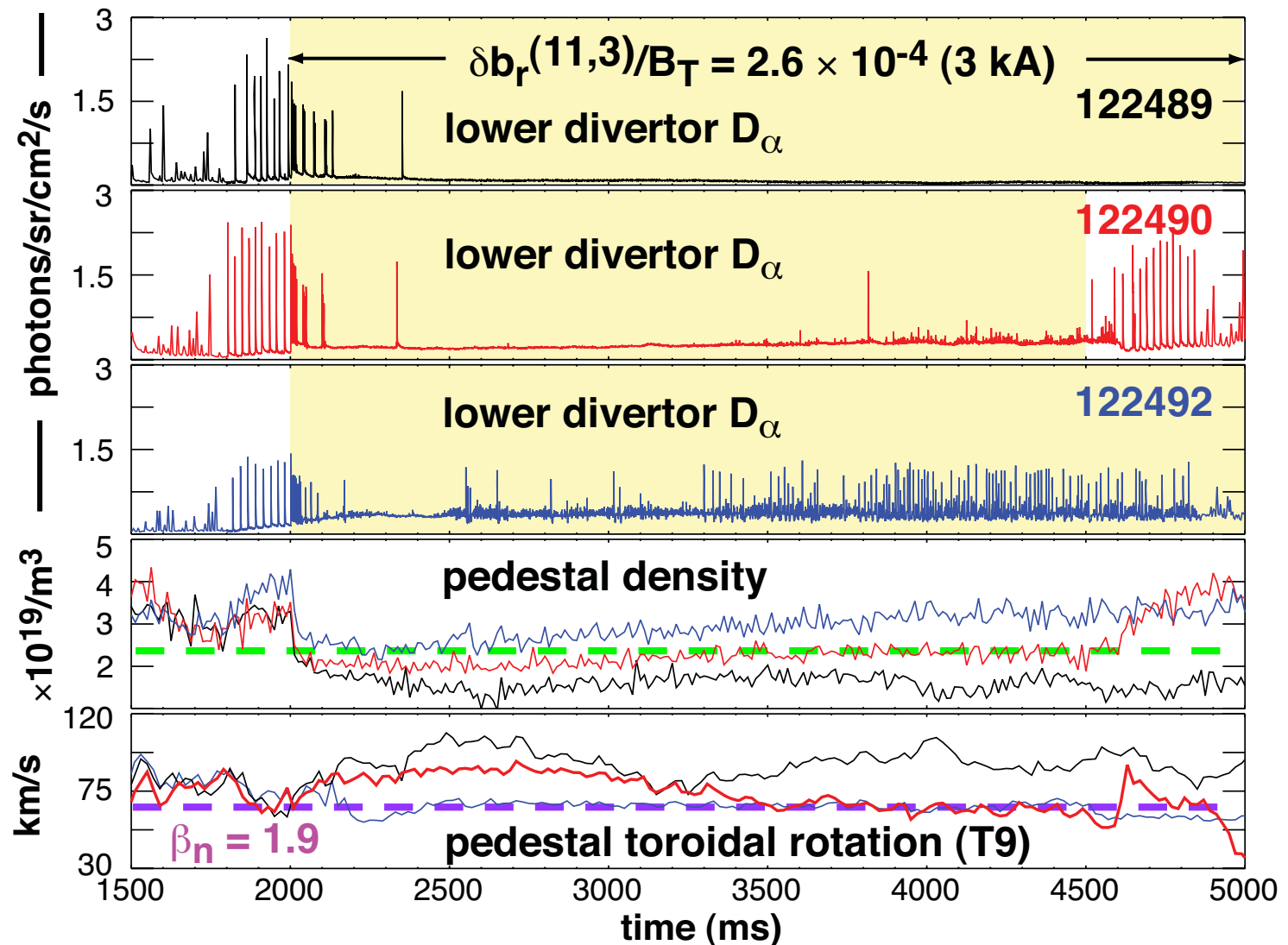
τ_p^* reduced a factor of 2 in pellet perturbation experiments with similar recycling ($\rightarrow \tau_p$ change)

- Identical pellets injected into discharges with $\nu_e^* \sim 0.2$, $\delta \sim 0.7$, and similar recycling conditions:
 - I-coil = 0 kA, ELMing H-mode
 - I-coil = 4 kA, RMP-assisted ELM-free H-mode



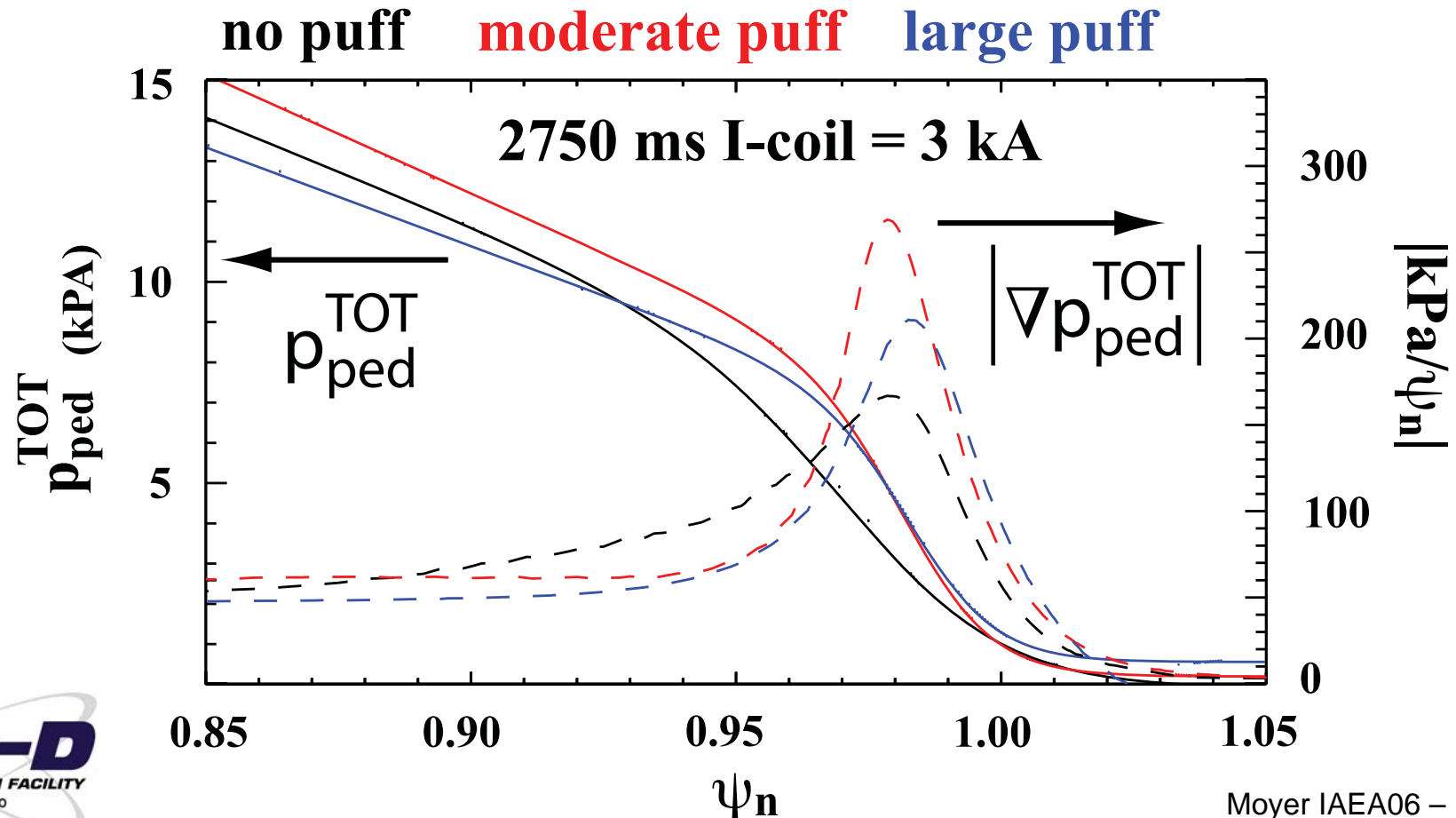
D2 puffing raises pedestal density in ELM-suppressed phase until a limit where small ELMs onset.

- Onset of small ELMs is correlated with **density upper limit** and **pedestal v_ϕ lower limit**.
- Density limit increases with RMP strength and neutral beam power
- Similar to weak RMP results at $v_e^* \sim 1$ but at $v_e^* \sim 0.15$



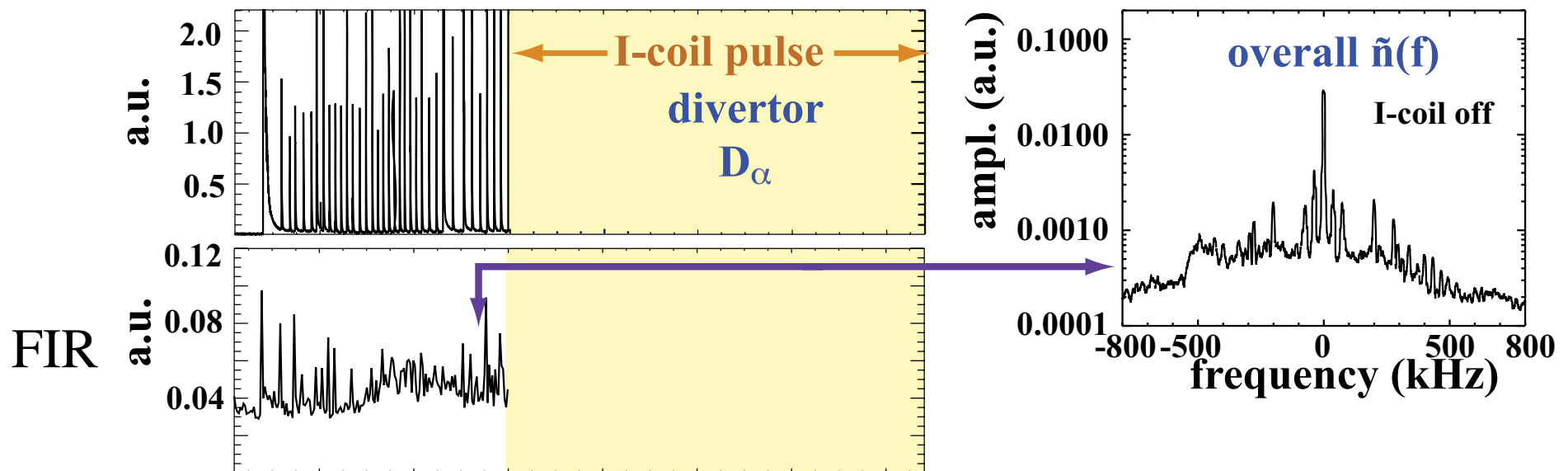
D2 puffing into RMP-assisted ELM-free H-mode raises $\nabla p_{\text{ped}}^{\text{TOT}}$ until $n=30$ P-B modes are destabilized.

- D2 puffing into RMP-assisted ELM-free H-mode gradually raises pedestal pressure and pressure gradient.
- Discharge becomes unstable to high $n=30$ P-B modes about the time that small ELMs/events onset during I-coil phase
- Small ELMs/events may be acceptable ITER operating regime.



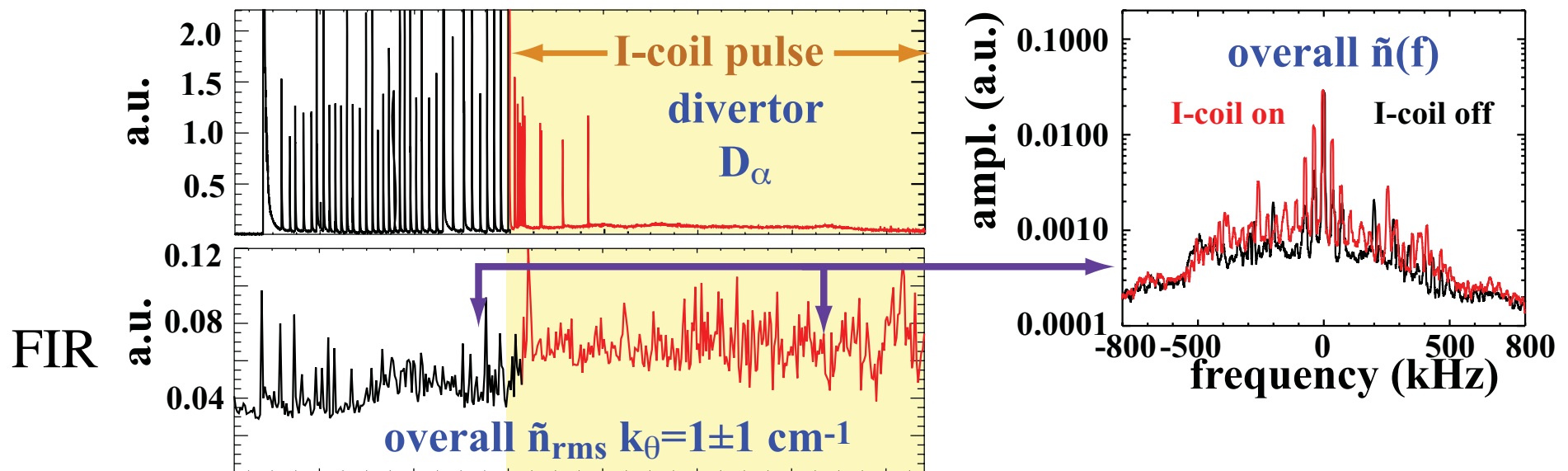
Increased particle transport during RMP may be due to increased fluctuation-driven transport.

- FIR scattering: $k_\theta = 1 \text{ cm}^{-1}$ not spatially localized



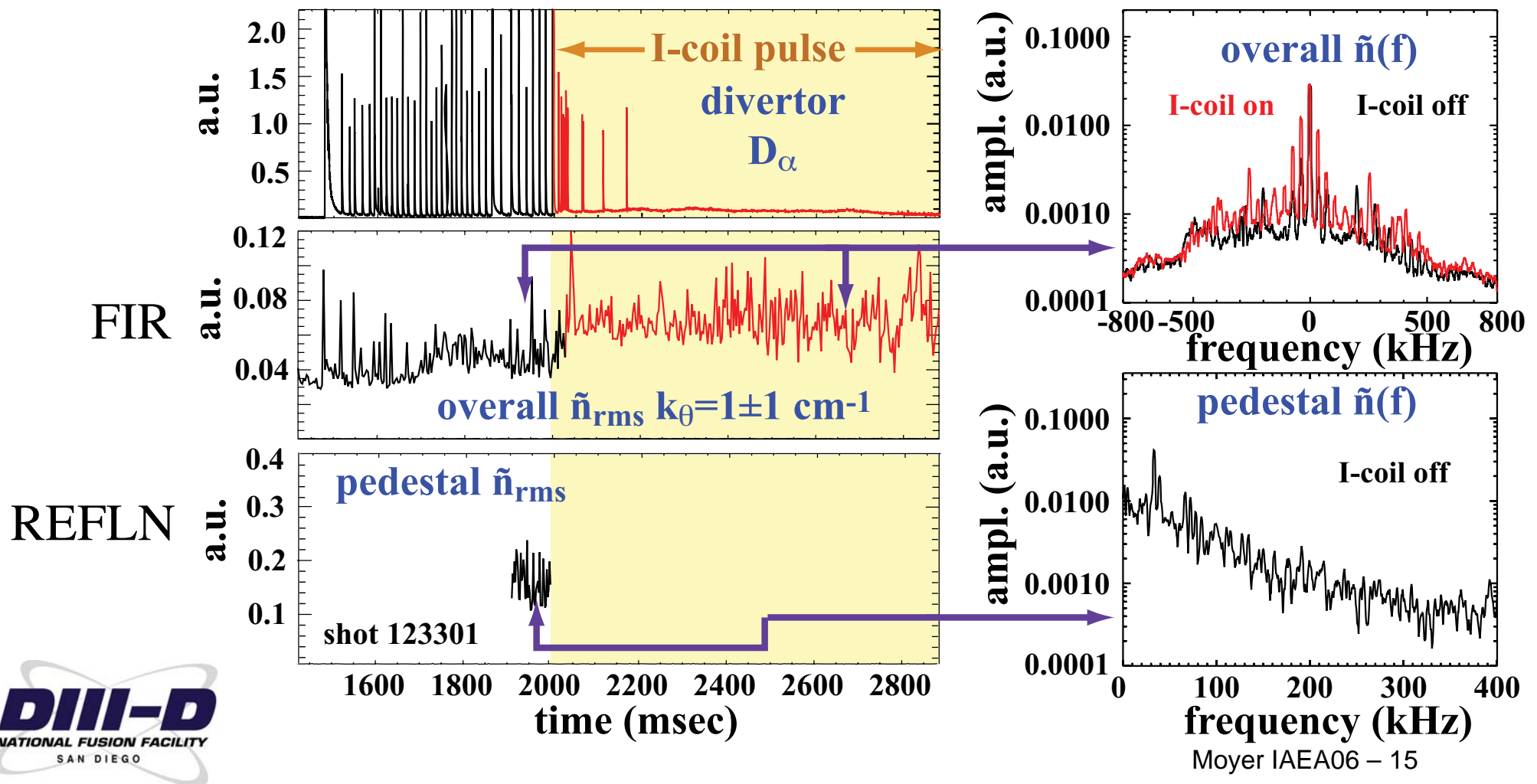
Increased particle transport during RMP may be due to increased fluctuation-driven transport.

- FIR scattering: $k_\theta = 1 \text{ cm}^{-1}$ not spatially localized \rightarrow increased coherent modes and broadband turbulence \rightarrow 1.5x increase in \tilde{n}_{rms}



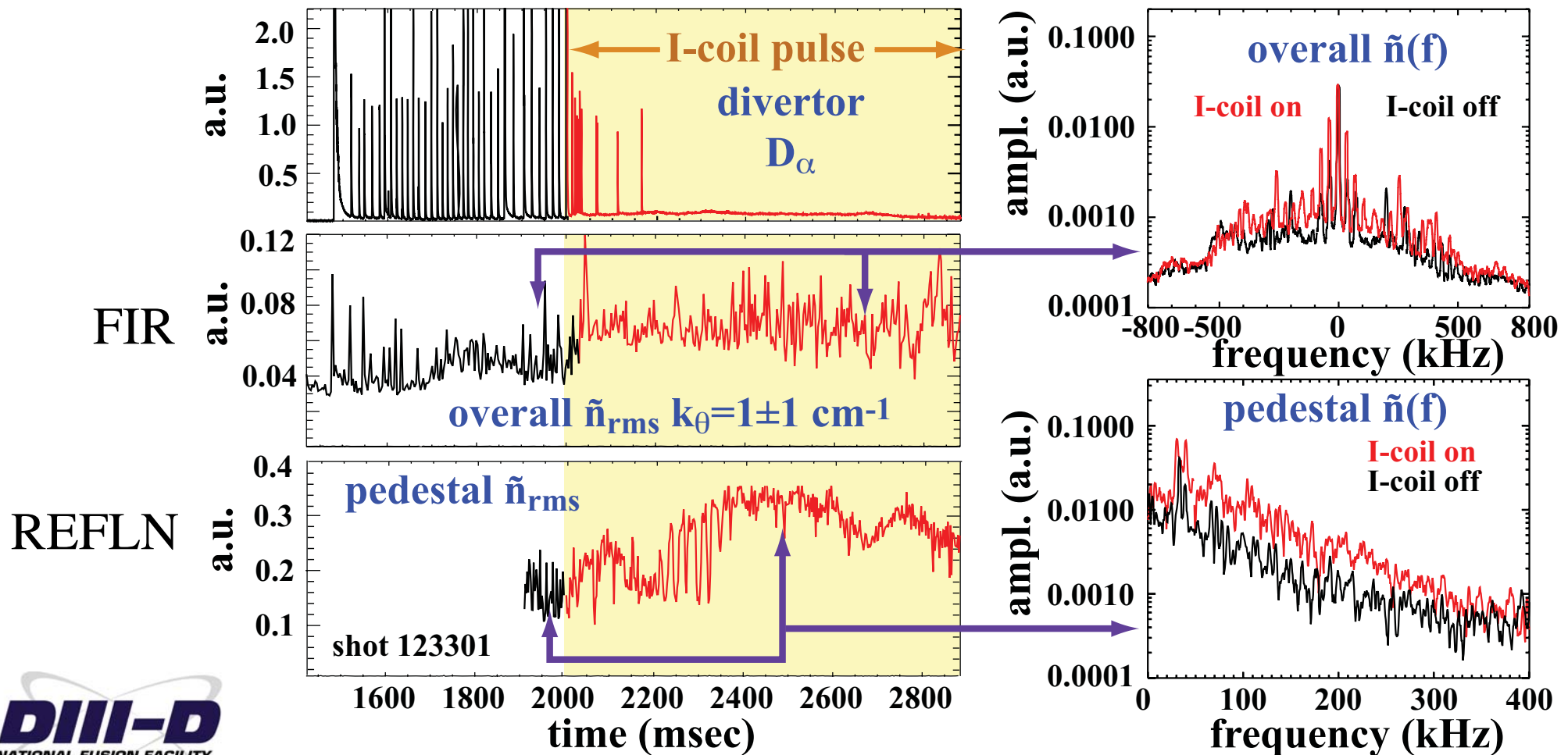
Increased particle transport during RMP may be due to increased fluctuation-driven transport.

- FIR scattering: $k_\theta = 1 \text{ cm}^{-1}$ not spatially localized \rightarrow increased coherent modes and broadband turbulence \rightarrow 1.5x increase in \tilde{n}_{rms}
- reflectometry: localized to pedestal



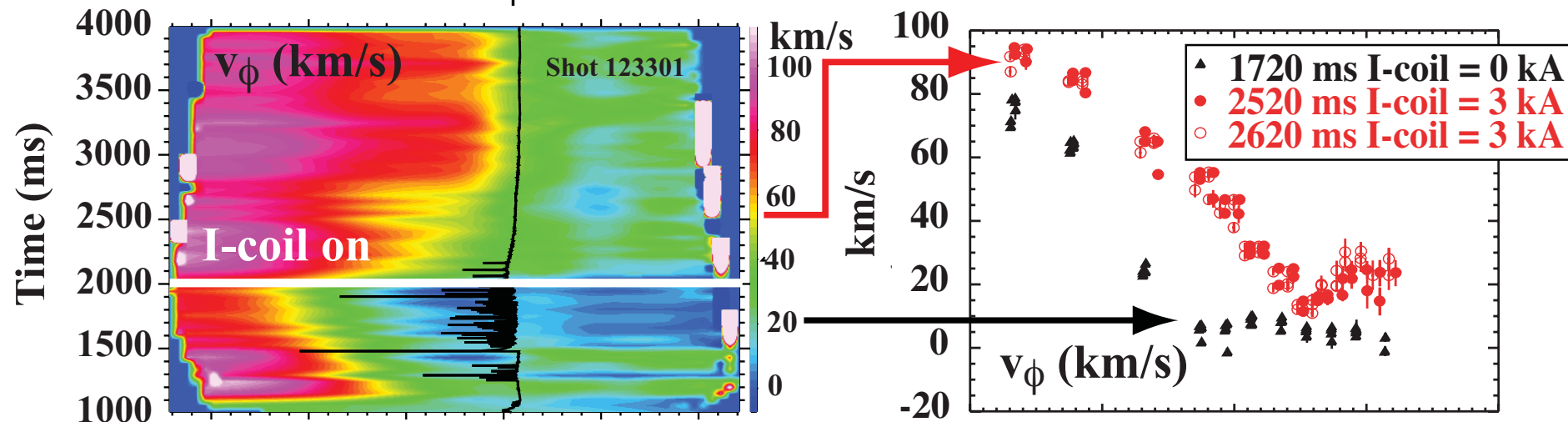
Increased particle transport during RMP may be due to increased fluctuation-driven transport.

- FIR scattering: $k_\theta = 1 \text{ cm}^{-1}$ not spatially localized \rightarrow increased coherent modes and broadband turbulence \rightarrow 1.5x increase in \tilde{n}_{rms}
- reflectometry: localized to pedestal \rightarrow increased turbulence \rightarrow 2x increase in \tilde{n}_{rms}
- $D_{\text{eff}} \sim \tilde{n}_{\text{rms}}^2 \rightarrow D_{\text{eff}}$ increases 3-4x, consistent with change inferred from profiles.



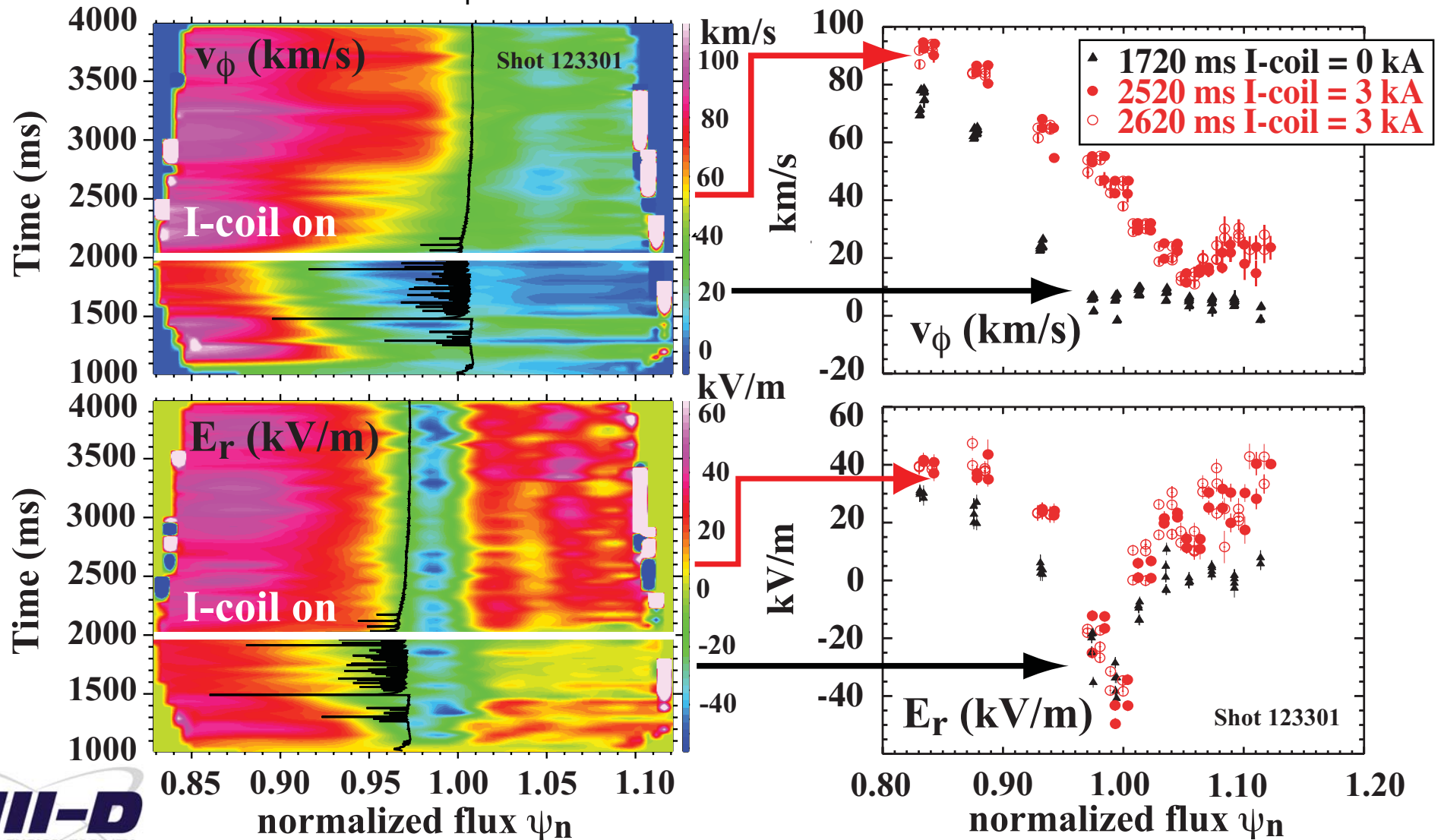
Pedestal toroidal rotation and E_r change promptly when RMP is applied and edge q resonant ($3.4 < q_{95} < 3.7$).

- H-mode pedestal v_ϕ spins up



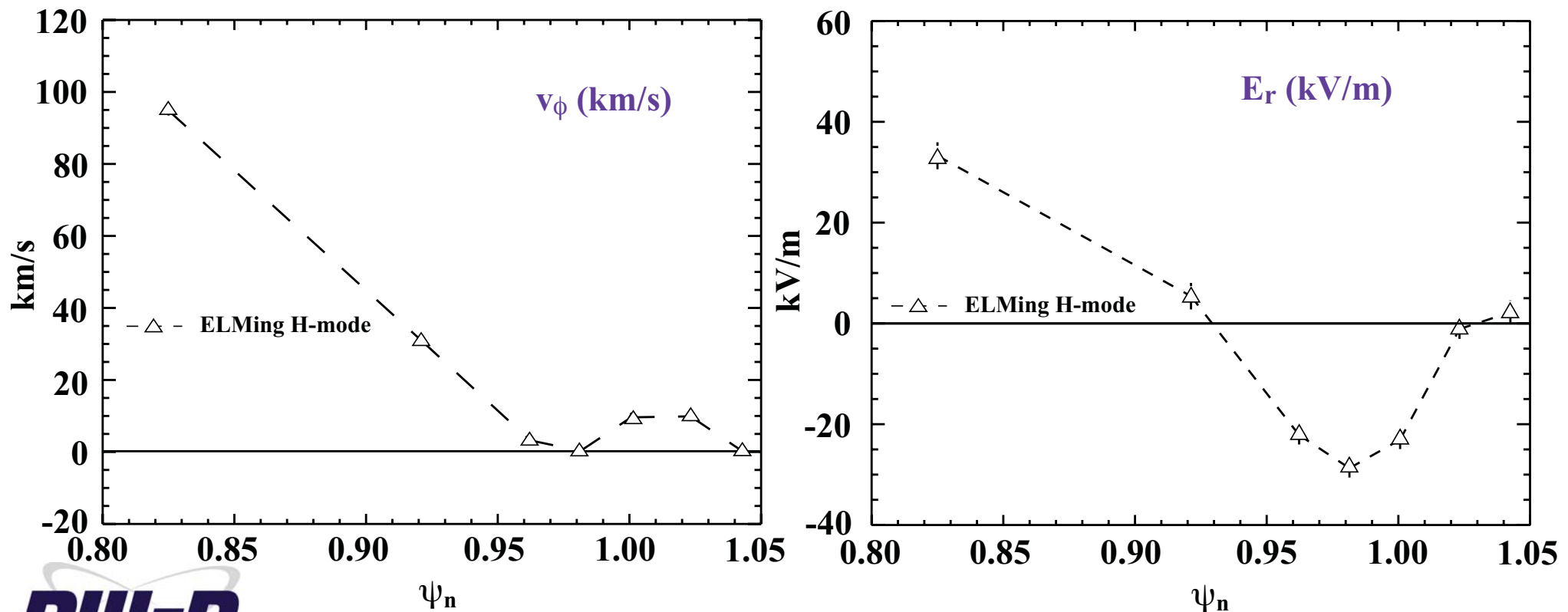
Pedestal toroidal rotation and E_r change promptly when RMP is applied and edge q resonant ($3.4 < q_{95} < 3.7$).

- H-mode pedestal v_ϕ spins up and E_r well narrows.



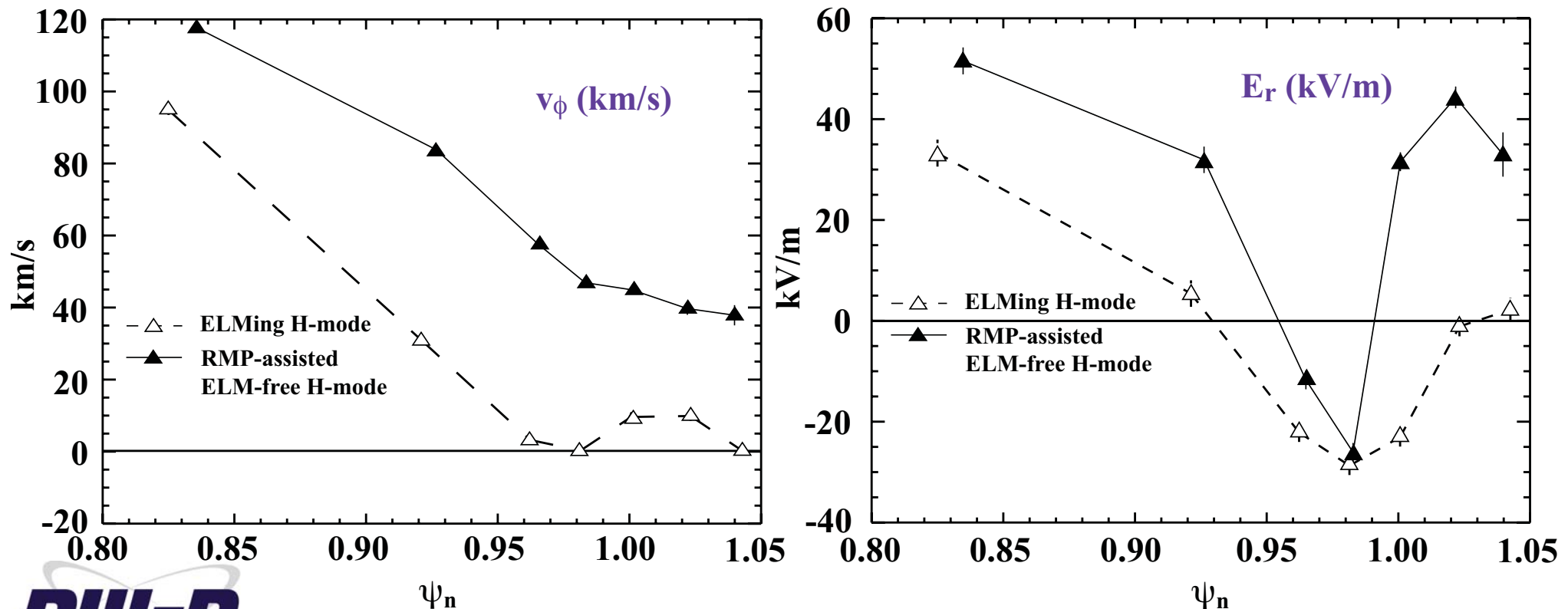
Onset of small ELMs as n_e^{ped} rises is correlated with decay of pedestal v_ϕ and degradation of E_r well.

- As n_e^{ped} rises, v_ϕ and E_r profiles become more like ELMing H-mode



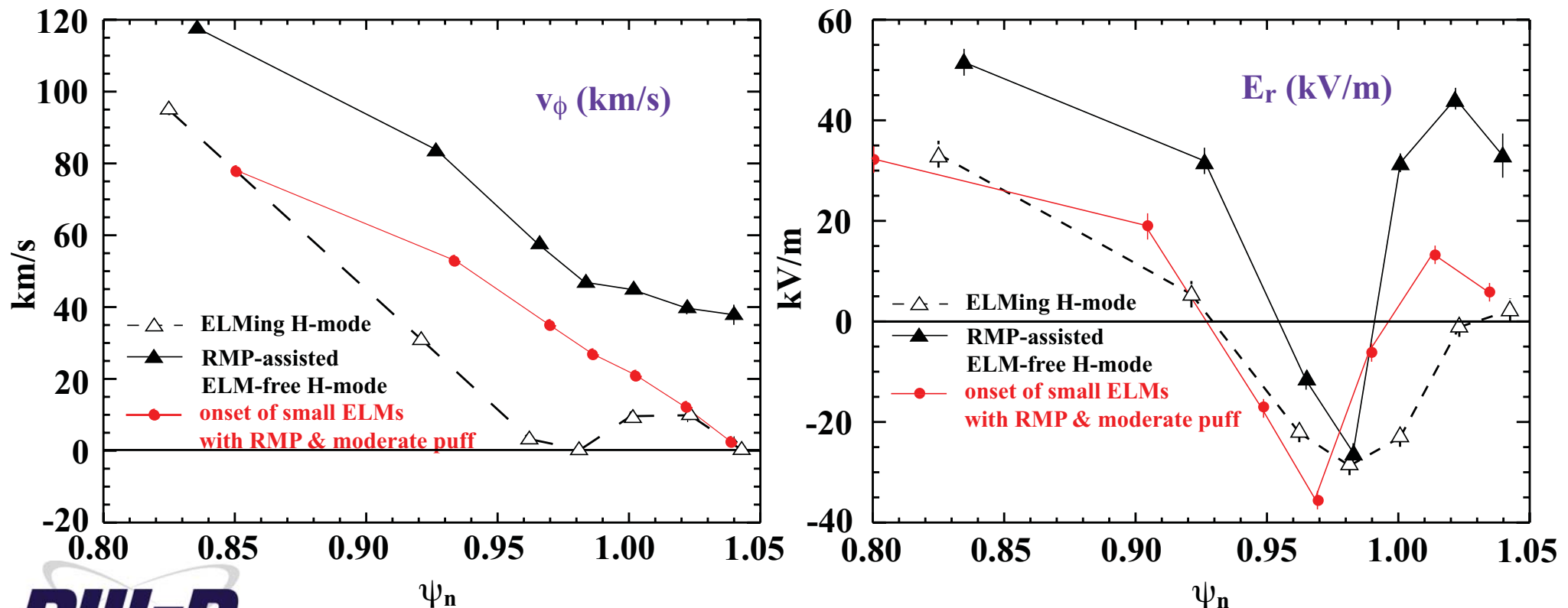
Onset of small ELMs as n_e^{ped} rises is correlated with decay of pedestal v_ϕ and degradation of E_r well.

- As n_e^{ped} rises, v_ϕ and E_r profiles become more like ELMy H-mode



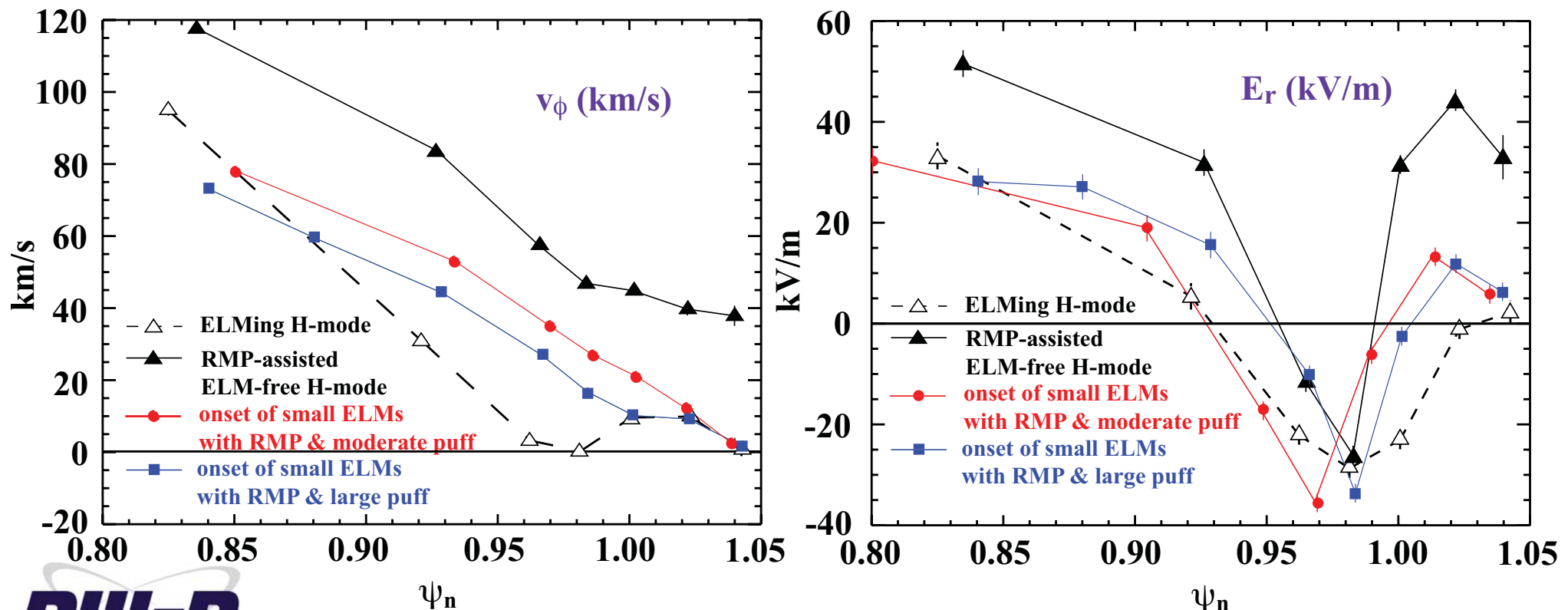
Onset of small ELMs as n_e^{ped} rises is correlated with decay of pedestal v_ϕ and degradation of E_r well.

- As n_e^{ped} rises, v_ϕ and E_r profiles become more like ELMing H-mode



Onset of small ELMs as n_e^{ped} rises is correlated with decay of pedestal v_ϕ and degradation of E_r well.

- As n_e^{ped} rises, v_ϕ and E_r profiles become more like ELMing H-mode
- Changes in v_ϕ and E_r are similar to those seen in RMP-assisted ELM-free H-mode at $v_e^* \sim 1$ which also displays small, rapid ELMs/events
- suggests that E_r /velocity shear changes may regulate the transport response to the RMP, and therefore the ELM stability by altering ∇p



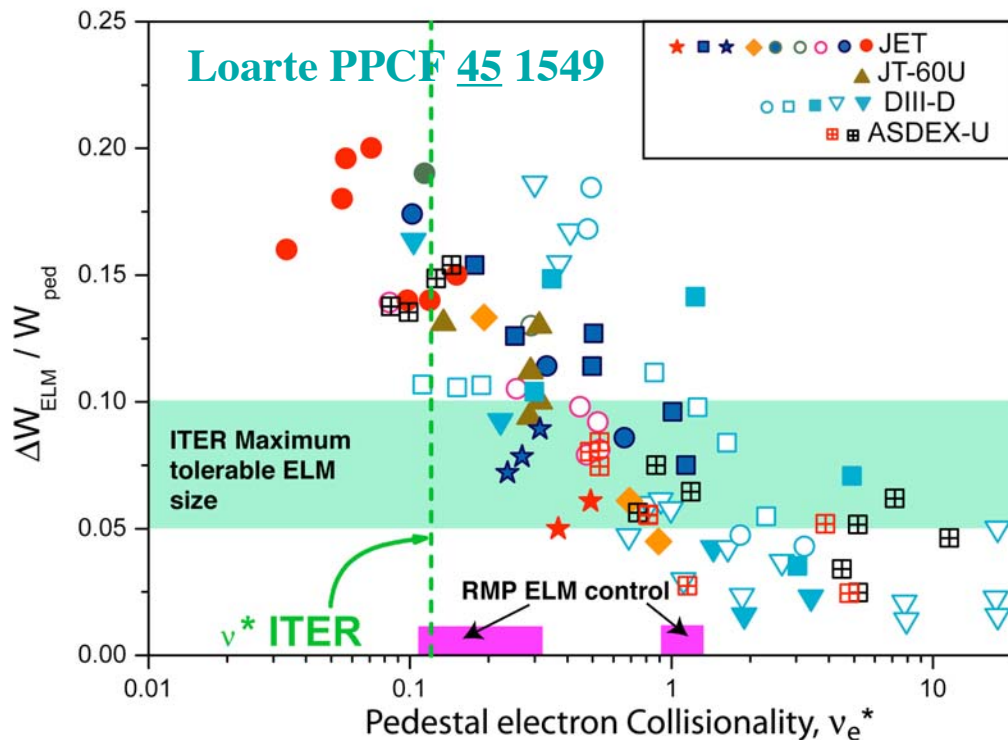
Summary and Conclusions

- Complete ELM suppression has been obtained in ELMy H-modes with ITER-relevant pedestal electron collisionality ν_e^* and ITER-similar shape (ISS) using an edge-resonant magnetic perturbation.
- ELMs are suppressed by lowering the pedestal pressure gradient below the Peeling-Ballooning stability limit for Type I ELMs.
- Pedestal pressure gradient reduction is controlled with RMP strength $\delta b_r^{m,n}/B_T$ above a shape-dependent minimum of 2.8×10^{-4} ($\delta \sim 0.37$) to 3.4×10^{-4} ($\delta \sim 0.7$).
- Pressure gradient is reduced primarily by RMP-induced particle transport.
- Density fluctuations increase 1.5-2x during RMP, consistent with increased convective particle transport.
 - Fluctuations may play similar role to Edge Harmonic Oscillation in QH-mode [[see P.B. Snyder, this meeting](#)]
 - $D_{\text{eff}} \sim n_{\text{rms}}^2$ increases 3-4x, consistent with density profile changes
 - Suggests that E_r /velocity shear changes due to RMP regulate transport, leading to reduced ∇p and stabilizing ELMs.

Backup Slides

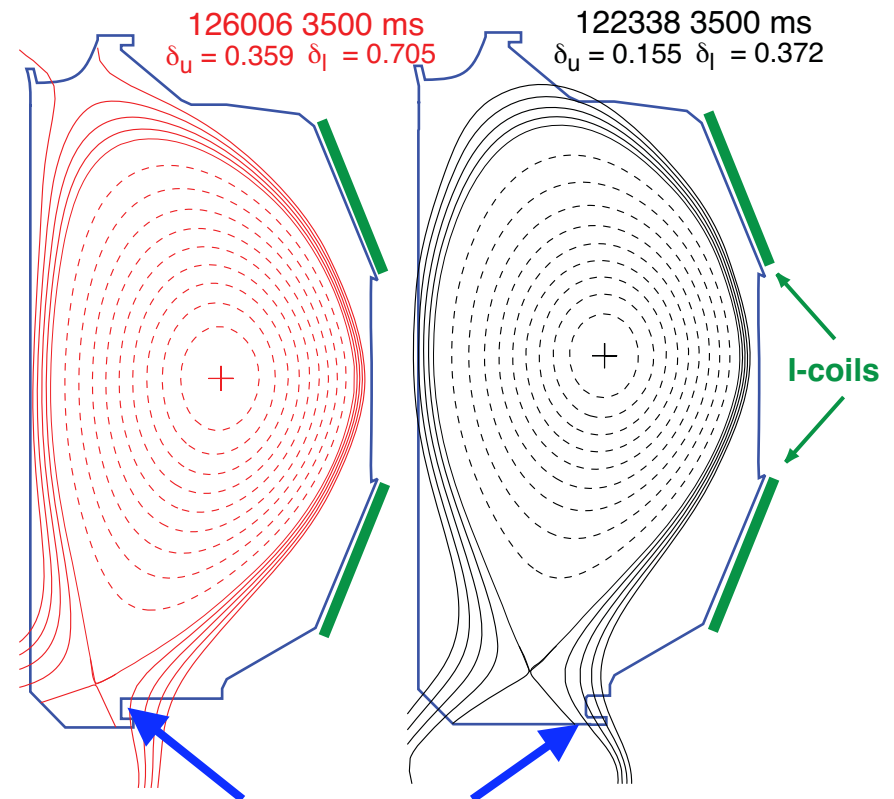
ELM control is a critical issue for burning plasmas.

- $\Delta W_{\text{ELM}}/W_{\text{PED}}$ increases as pedestal collisionality ν_e^* drops



- RMP penetration decreases at lower ν_e^*
- Parallel transport increases at lower ν_e^*

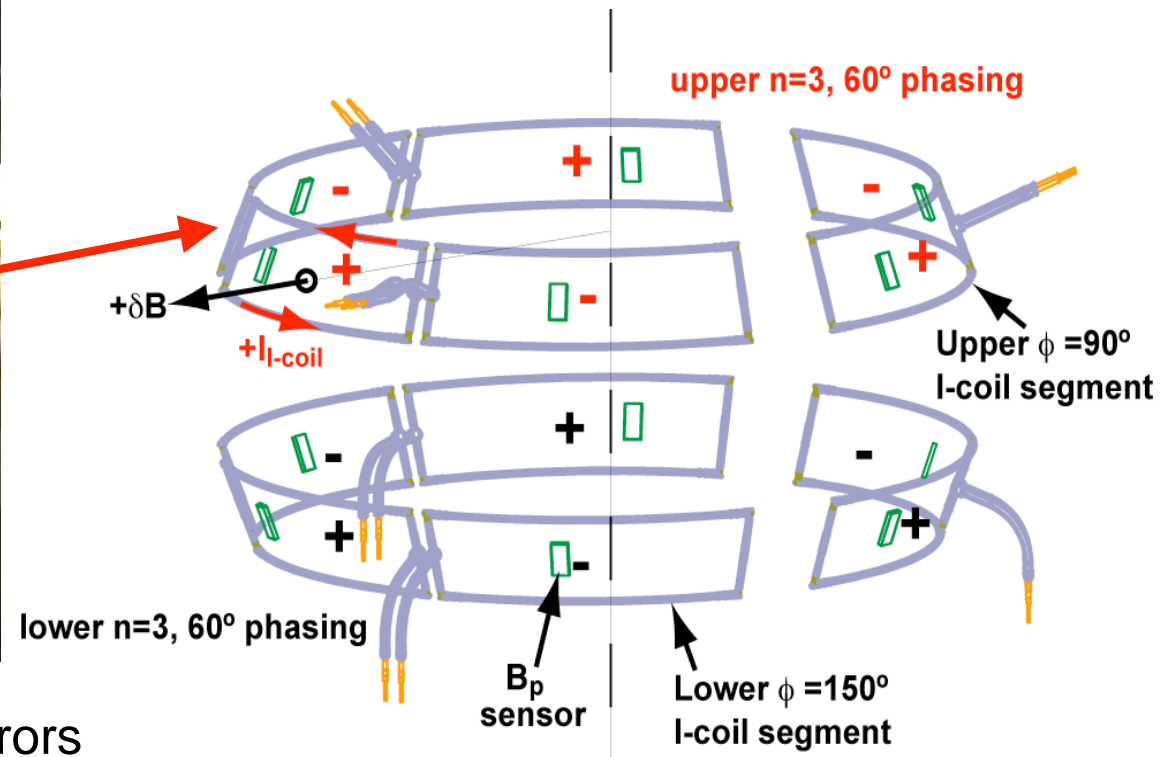
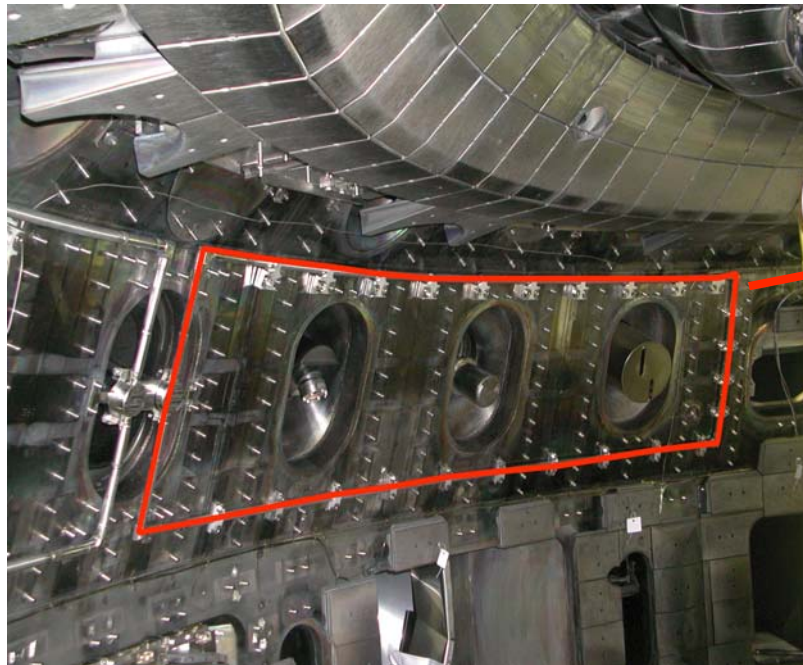
- ITER pedestal ν_e^* achieved in DIII-D by divertor pumping



- New lower divertor (2006) enables pumping high δ lower divertor to achieve ITER-relevant ν_e^*

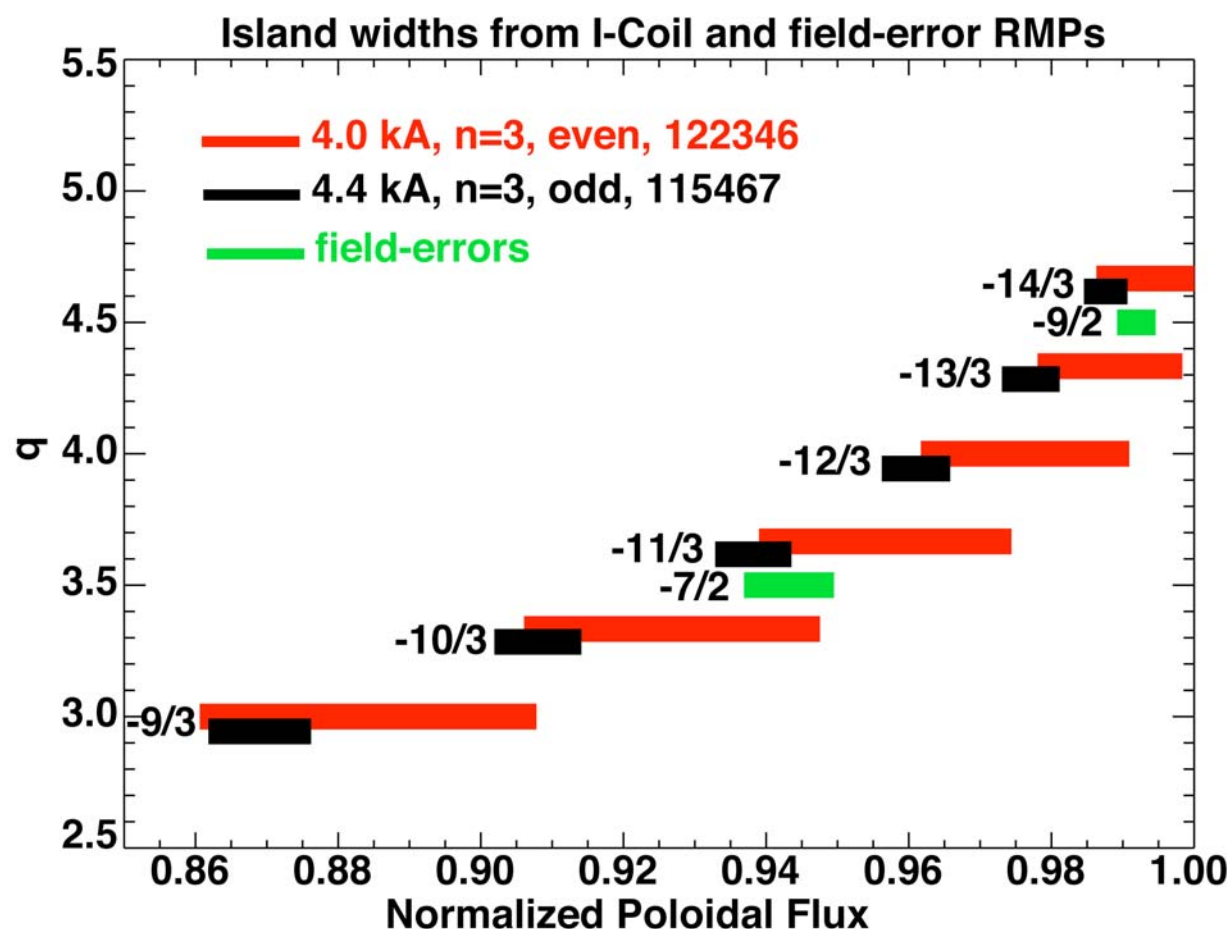
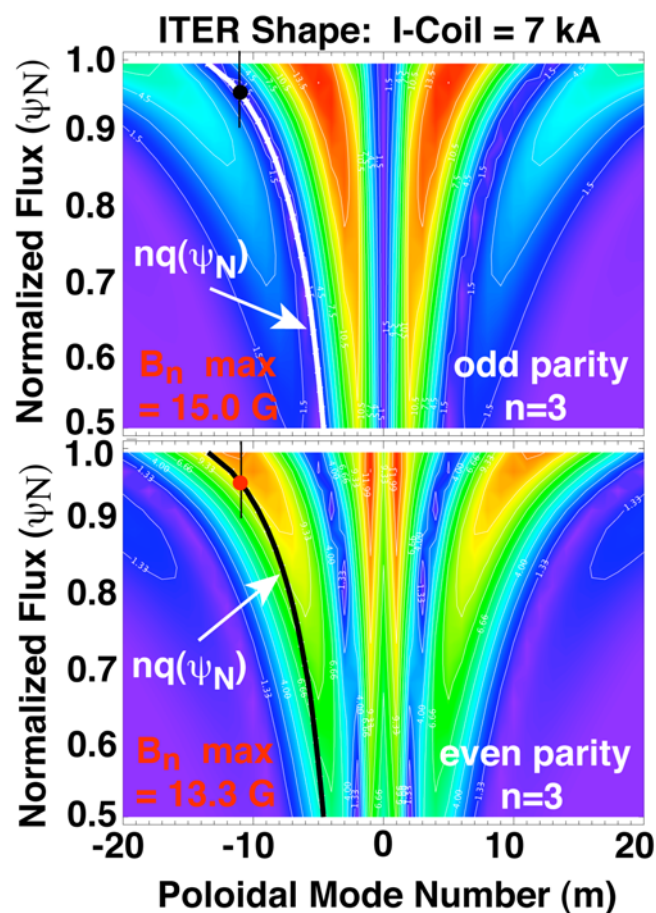
The DIII-D I-coil provides a flexible system for $n=3$ ELM control experiments

- $n = 3$ used to minimize core perturbations.
- $9 < m < 15$ Fourier harmonics form edge stochastic layer.



- Mixing with fixed intrinsic field errors
 - $\phi_{\text{tor}} = 0^\circ$ or 60° gives different levels of stochasticity
 - δB_r for segment pairs in the same or opposite direction ("even" & "odd" parity)
 - Can use $n=3$ C-coil perturbation to boost $n=3 \delta b_r^{3,m}$

I-coil parity controls pedestal island overlap

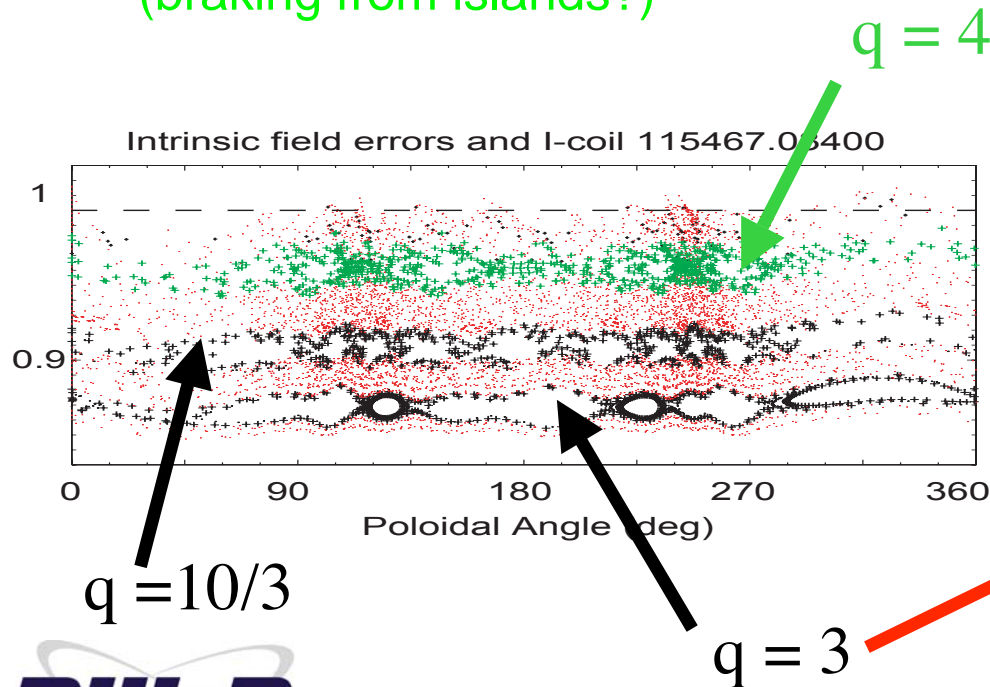


- Both parities suppress ELMs
 - Odd (weak RMP) → small islands → little or no change in pedestal
 - Even (strong RMP) → stochastic → transport / pedestal control

I-coil parity controls level of island overlap and stochasticity.

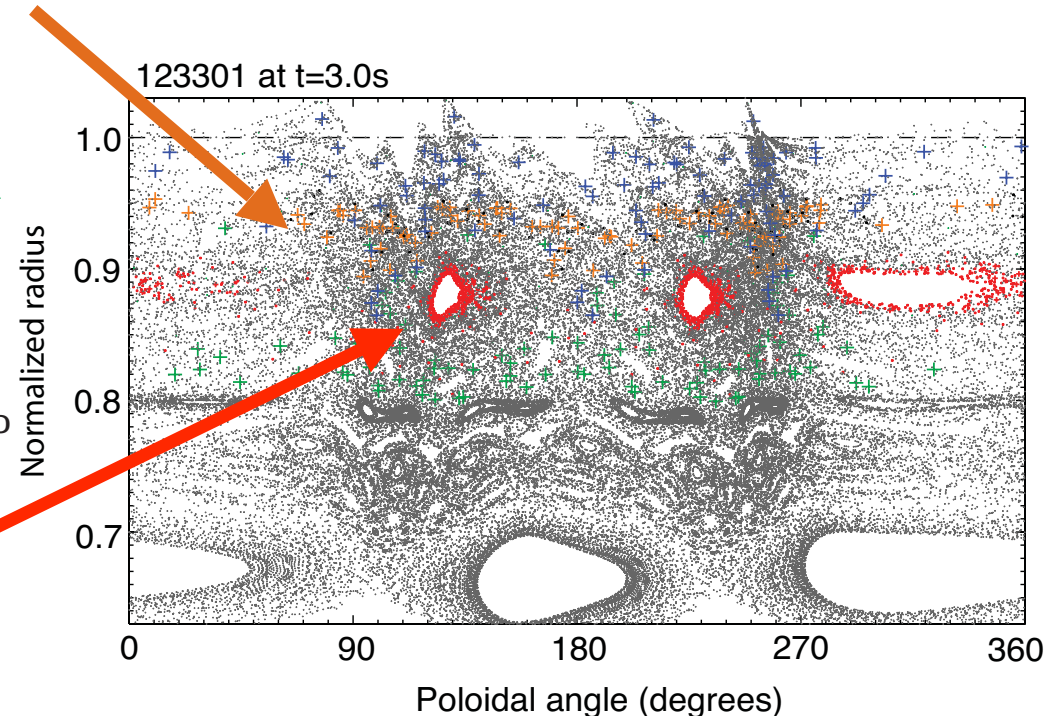
Moderate collisionality $\nu_e^* \geq 1$

- remnant islands mix with field error spectra
 - resonances at $q=3$, $10/3$, & 4 with evidence for higher harmonics
- Edge toroidal rotation drops (braking from islands?)



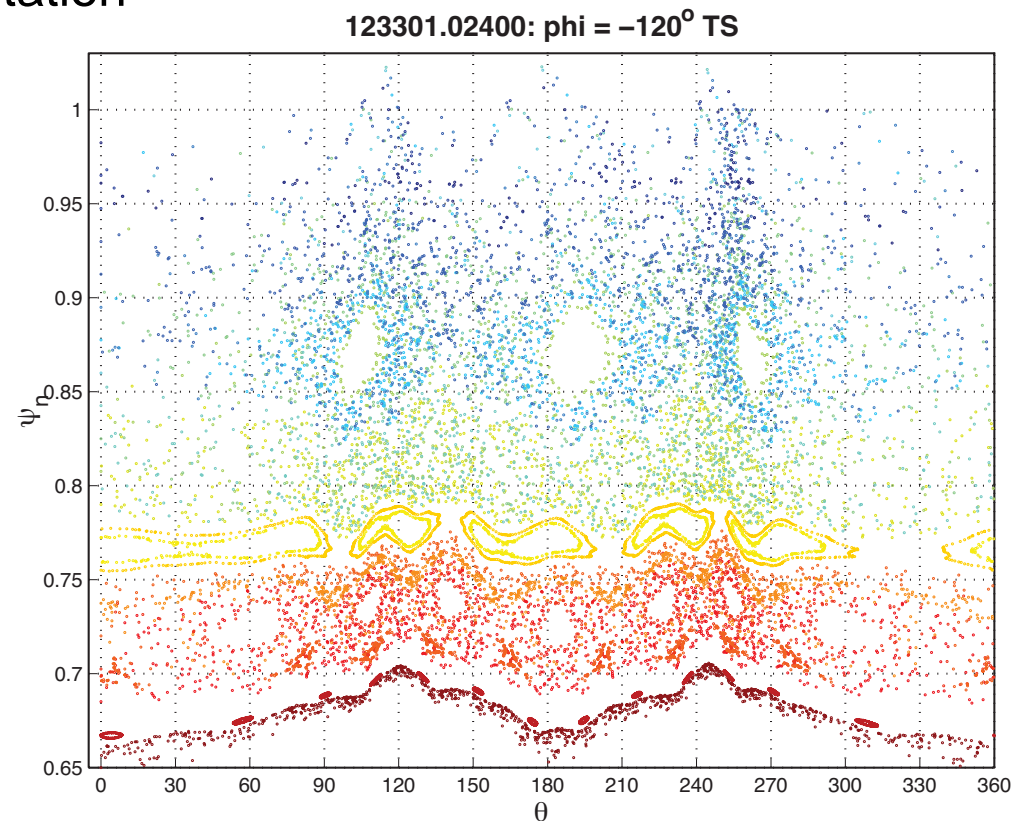
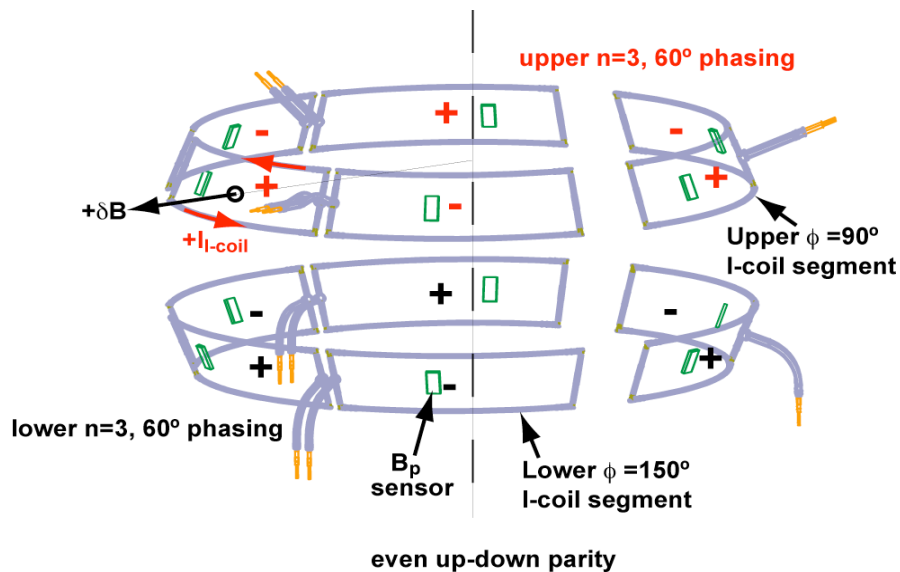
Low collisionality $\nu_e^* \sim 0.1$

- Pedestal is substantially more stochastic
 - Remnant island at $q=3$ nearly destroyed
 - Remnant islands at $q=10/3$, 4 completely destroyed
- Less drag because of randomness of field line orientation?

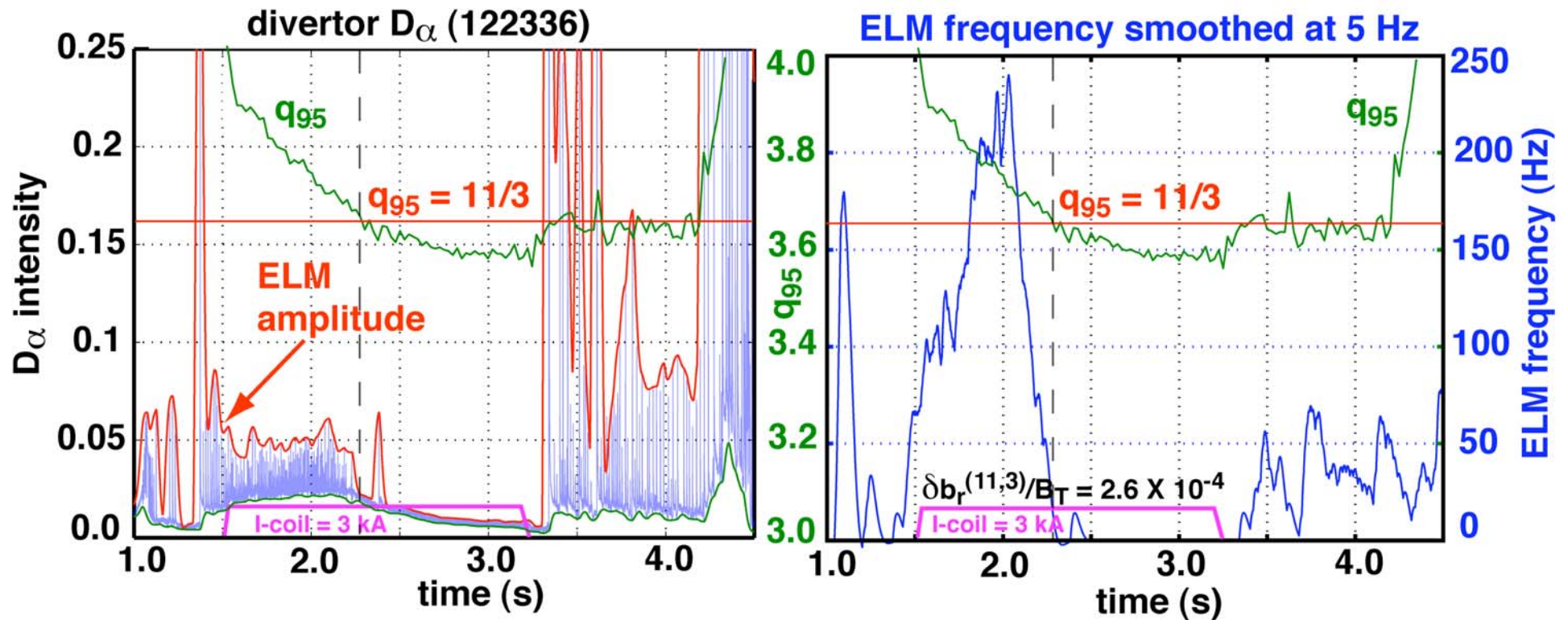


The DIII-D I-coil provides a flexible system for $n=3$ ELM control experiments

- I-coil parity controls pedestal island overlap
 - Odd (weak RMP) \rightarrow small islands \rightarrow little or no change in pedestal
 - Even (strong RMP) \rightarrow stochastic \rightarrow transport / pedestal control
- We focus on $n=3$ even parity \rightarrow strong edge resonant harmonics
 - Vacuum field island widths indicate overlap over plasma boundary in the absence of screening by beta or rotation

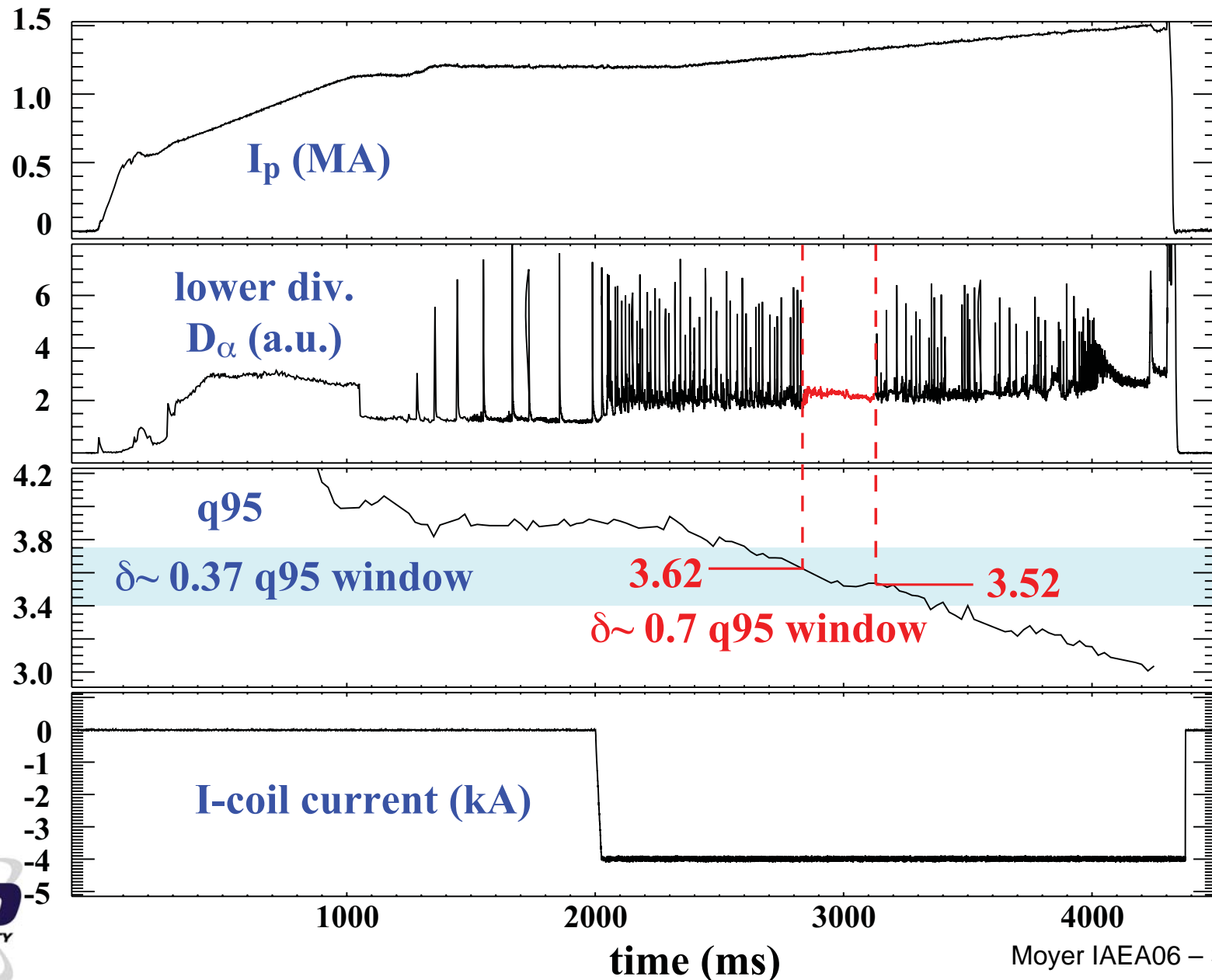


ELMs eliminated when resonant q_{95} condition satisfied with $\delta_{\text{lower}} = 0.36$ & $v_e^* \sim 0.1$



- $4.0 > q_{95} > 3.7 \rightarrow$ small, high frequency ELMs \rightarrow no large impulses
- $3.7 > q_{95} > 3.4 \rightarrow$ no ELMs
- Following RMP pulse large ELMs return with $\sim 250 \text{ ms}$ delay

q_{95} resonant window in ITER Similar Shape (ISS)
with $\delta_{\text{lower}} = 0.7$ is narrower than for $\delta_{\text{lower}} = 0.37$.



Transport regimes depend on ordering of λ_{mfp} , L_{corr} , L_{wall} (Rechester-Rosenbluth)

- Stochastic layer: collisionless transport
 - long field lines, stochasticity dominant

$$L_{corr} \ll \lambda_{mfp}, L_{wall} \quad D_{RR} = D_{st} v_{th}$$

- Stochastic layer: collisional transport (fluid limit)
 - long field lines, both stochasticity & collisions active

$$\lambda_{mfp} \ll L_{corr} \ll L_{wall} \quad \chi_{RR} = D_{st} \chi_{||} / L_{corr}$$

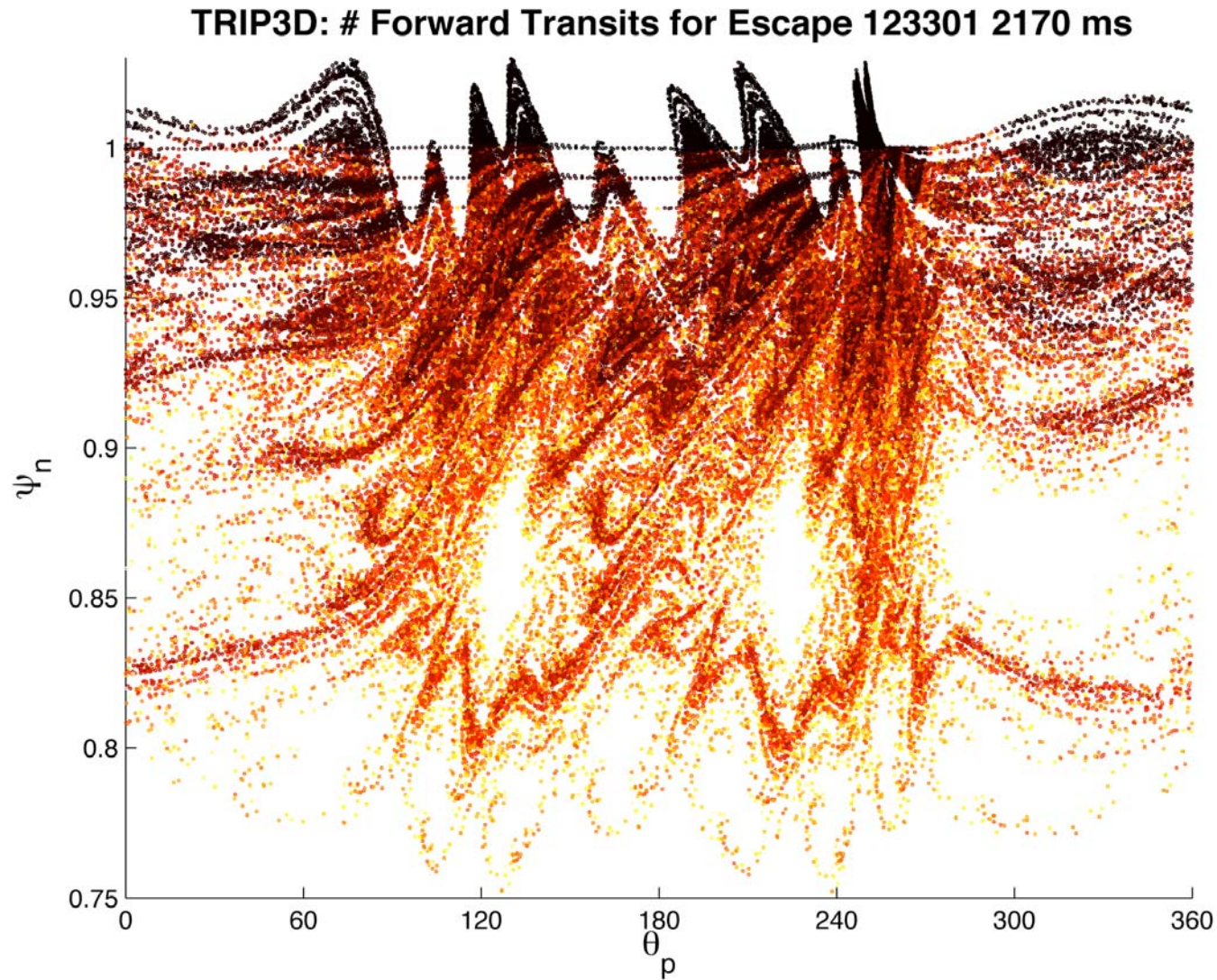
- SOL: collisional transport (fluid limit)
 - short field lines, collisions dominant

$$\lambda_{mfp} \ll L_{wall} \ll L_{corr} \quad \frac{L_{\perp}}{L_{wall}} = \sqrt{\frac{\chi_{\perp}}{\chi_{||}}}$$

- SOL: collisionless parallel transport
 - very short field lines

$$L_w \ll \lambda_{mfp}, L_c \quad \frac{L_{\perp}}{L_{wall}} = \sqrt{\frac{\chi_{\perp}}{L_{wall} v_{th}}} = \sqrt{\frac{\lambda_{mfp} \chi_{\perp}}{L_{wall} \chi_{||}}}$$

RMP induces magnetic diffusion and fractal structure in outer stochastic layer



- Color = # toroidal transits for escape (red=201 max, black<10)

E3D: 2 fluid transport code for ergodic 3D fields

see A.M. Runov P1-63 2006 PSI Mtg. (JNM in press 2007)

Solves Braginskii fluid equations in static background field

- Energy equation:

$$\frac{3}{2} n (\partial_t T + u_{\parallel} \nabla_{\parallel} T) = \nabla_{\parallel} \kappa_{\parallel} \nabla_{\parallel} T + \nabla_{\perp} \kappa_{\text{anom}} \nabla_{\perp} T - \Pi_{\parallel} \nabla_{\parallel} u_{\parallel} + Q_{\alpha\beta}$$

- Parallel momentum: **(alpha testing)**

$$mn \left(\partial_t u_{\parallel} + \nabla_{\parallel} \frac{u_{\parallel}^2}{2} \right) = q E_{\parallel} - \nabla_{\parallel} p + \Pi_{\parallel} + \Pi_{\text{anom}}$$

- Continuity: **(quasineutral)**

$$\partial_t n + \nabla_{\parallel} n u_{\parallel} = \nabla D_{\text{anom}} \nabla n$$

- Sheath BC's: **(nonlinear, R. Chodura)**

$$\Gamma = n C_s \cos \theta_w \sim n T^{1/2} \quad Q = \beta n T C_s \cos \theta_w \sim n T^{3/2}$$

E3D: efficient *Monte-Carlo* 2 fluid code designed for TEXTOR DED, W7-X, etc.

- **Heat transport highly anisotropic**

$$\kappa_{\parallel} / \kappa_{\perp} = \chi_{\parallel} / \chi_{\perp} \sim 10^8 - 10^{10}$$

- Stochasticity can generate small scales

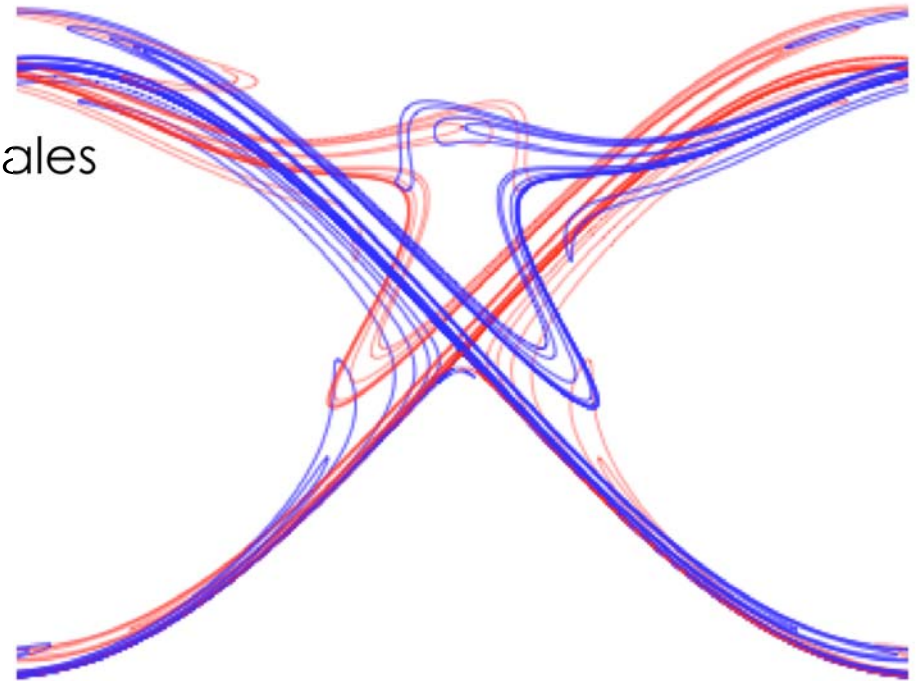
$$\ell_{\perp} / L_c \sim \sqrt{\chi_{\perp} / \chi_{\parallel}} \sim 10^{-4} - 10^{-5}$$

- **Simple finite elements cannot capture anisotropy**

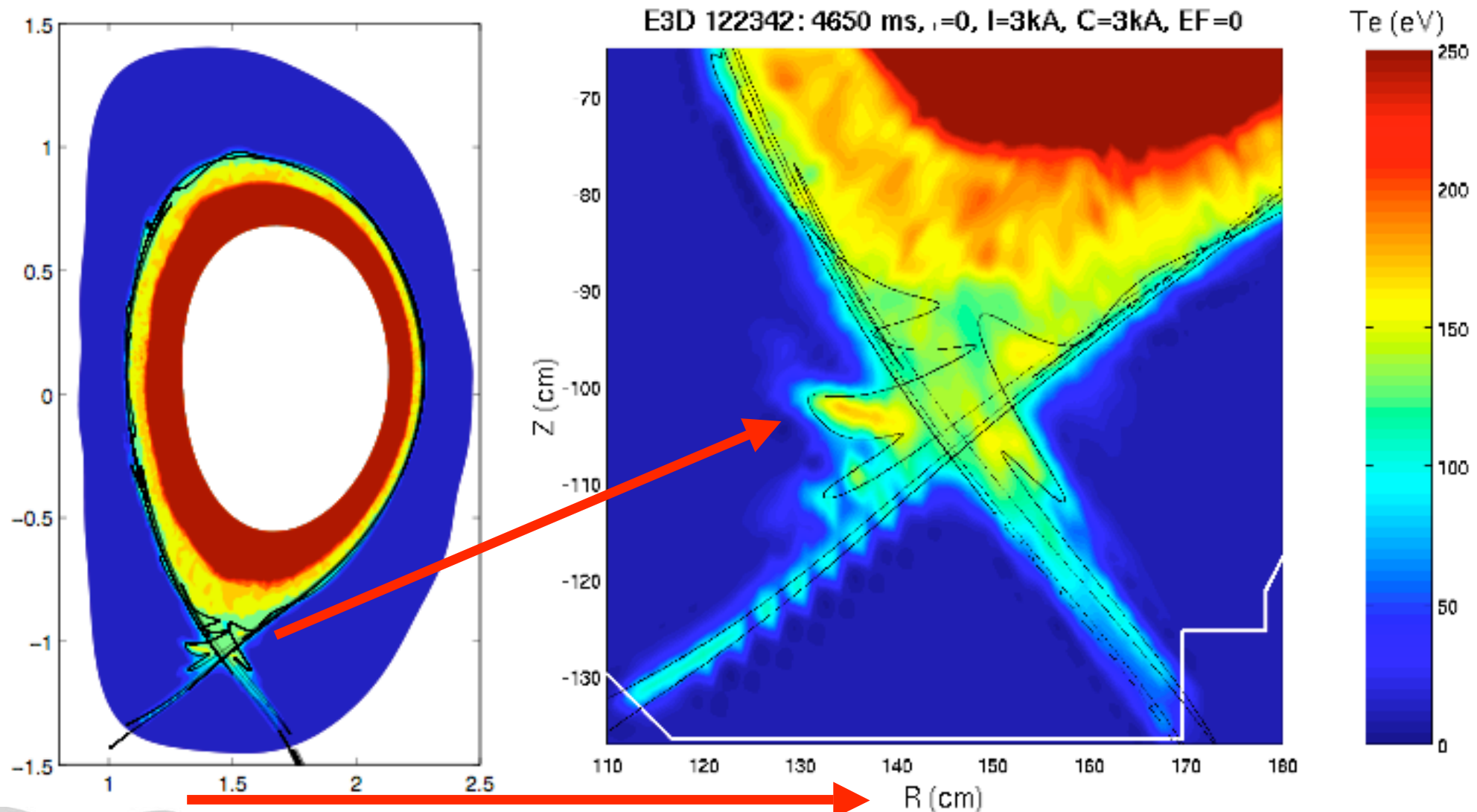
- Requires high order/adaptive
- May not capture 3D complexity

- **Solution: Monte-Carlo technique**

- Let $T(x,t)$ = *probability distribution function* for heat packets
- Use Brownian motion to describe evolution

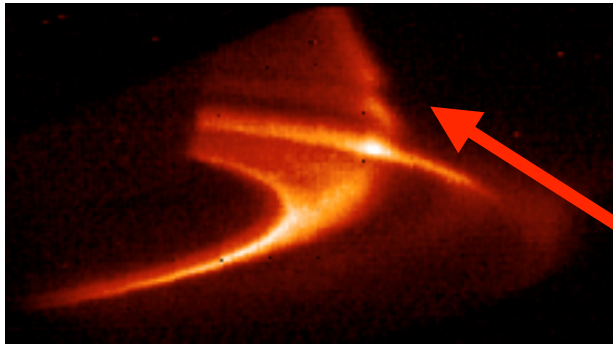


T_e profile follows homoclinic tangle
“Separatrix” = intersection of invariant manifolds

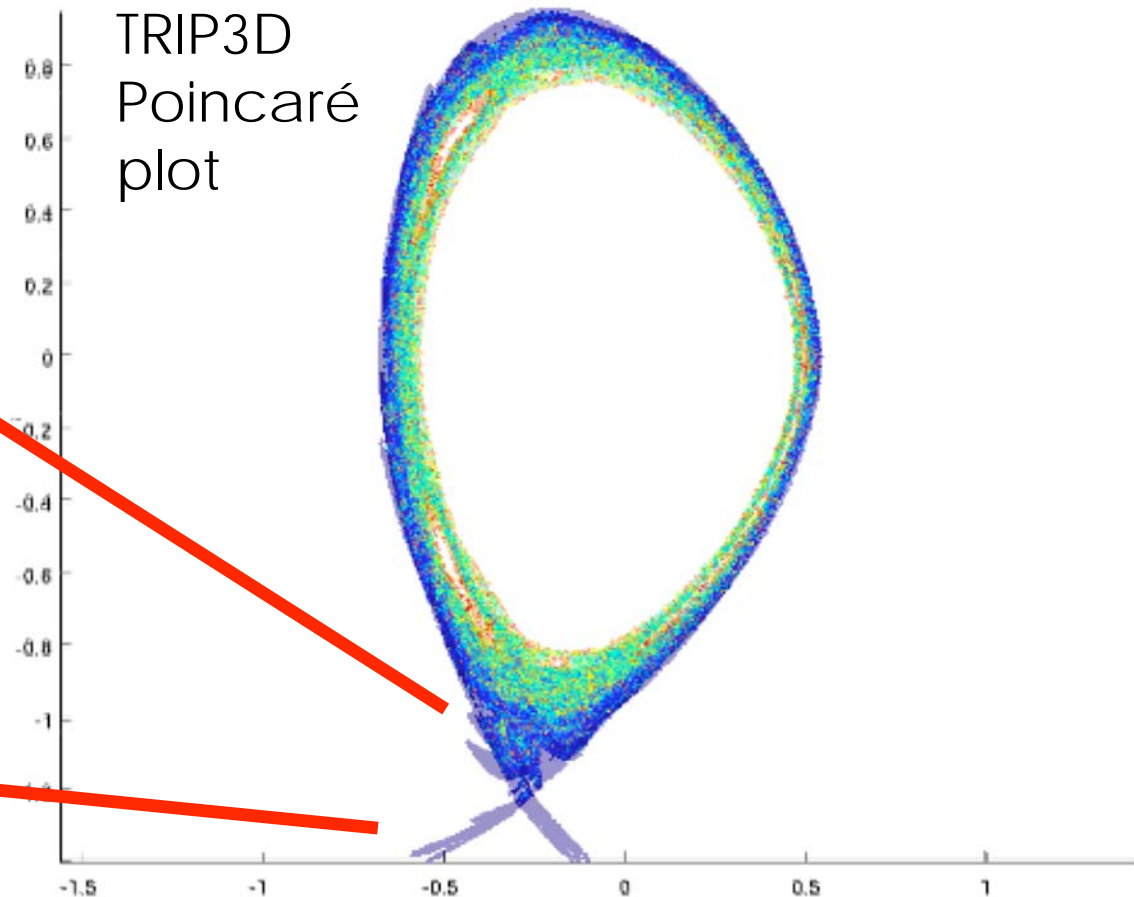
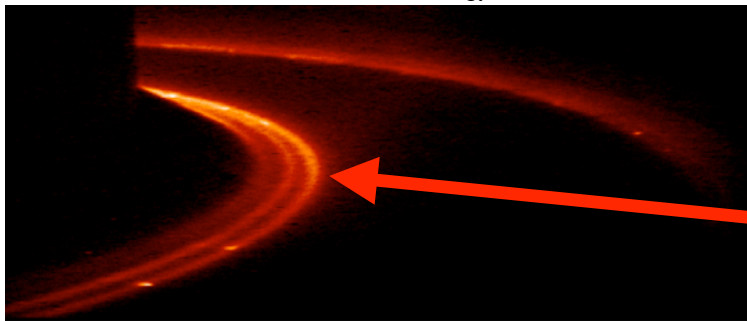


Xpt-TV experimental observations of “homoclinic tangle” confirm penetration of RMP at least into last few % in ψ_n .

123300: filtered CIII Xpt-TV



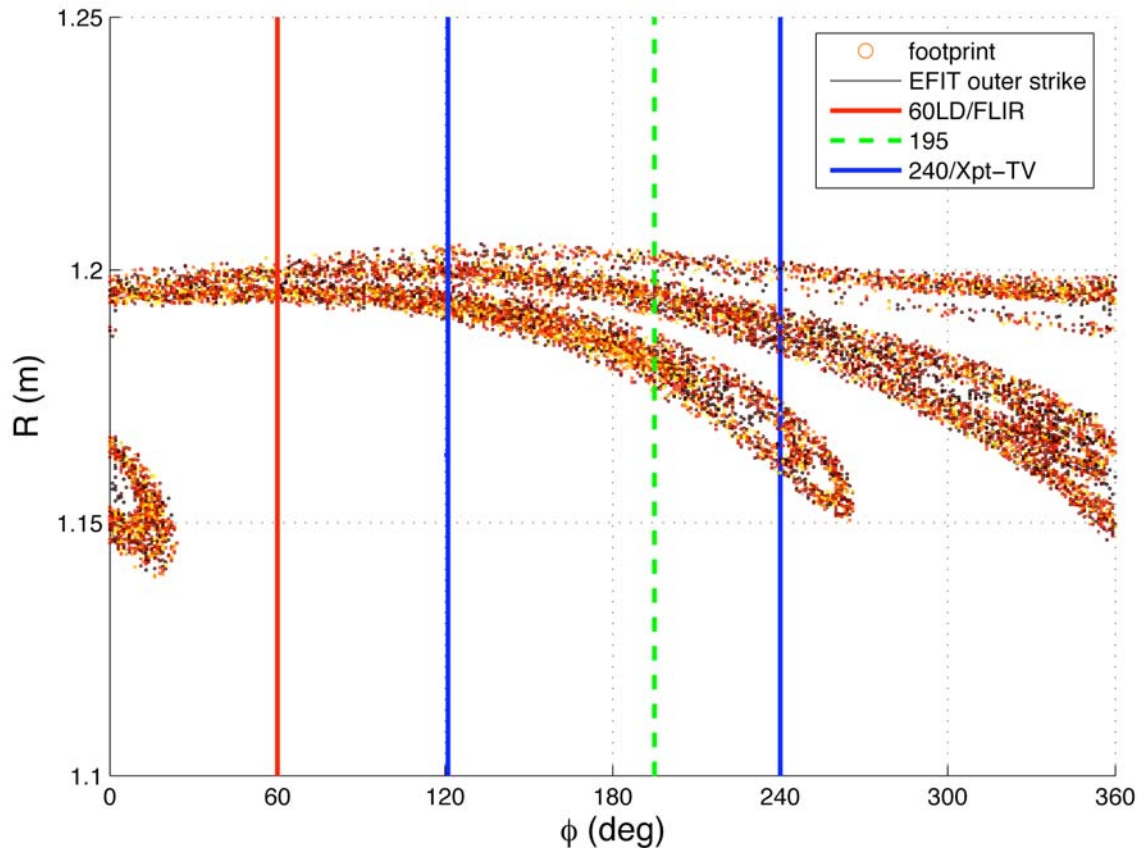
123301: filtered D_α Xpt-TV



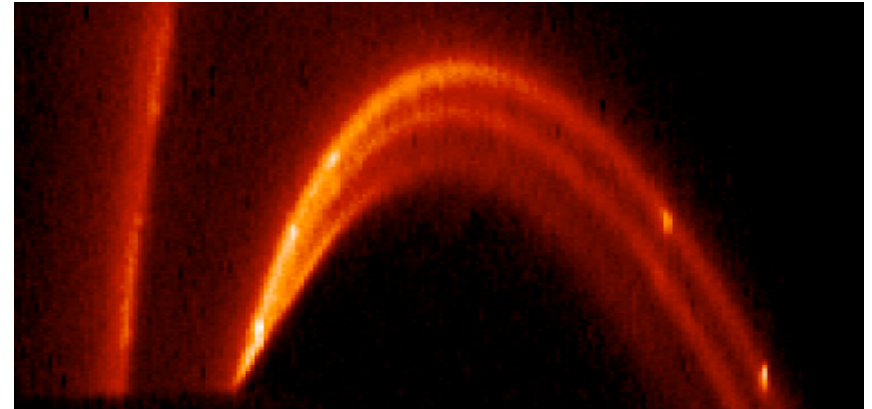
- T_e should reflect a superposition of both invariant manifolds
- Divertor plate striations often observed in experiment

Magnetic footprint striations often observed during I-coil pulse

TRIP3D prediction:
123301 2170 ms inner strike point



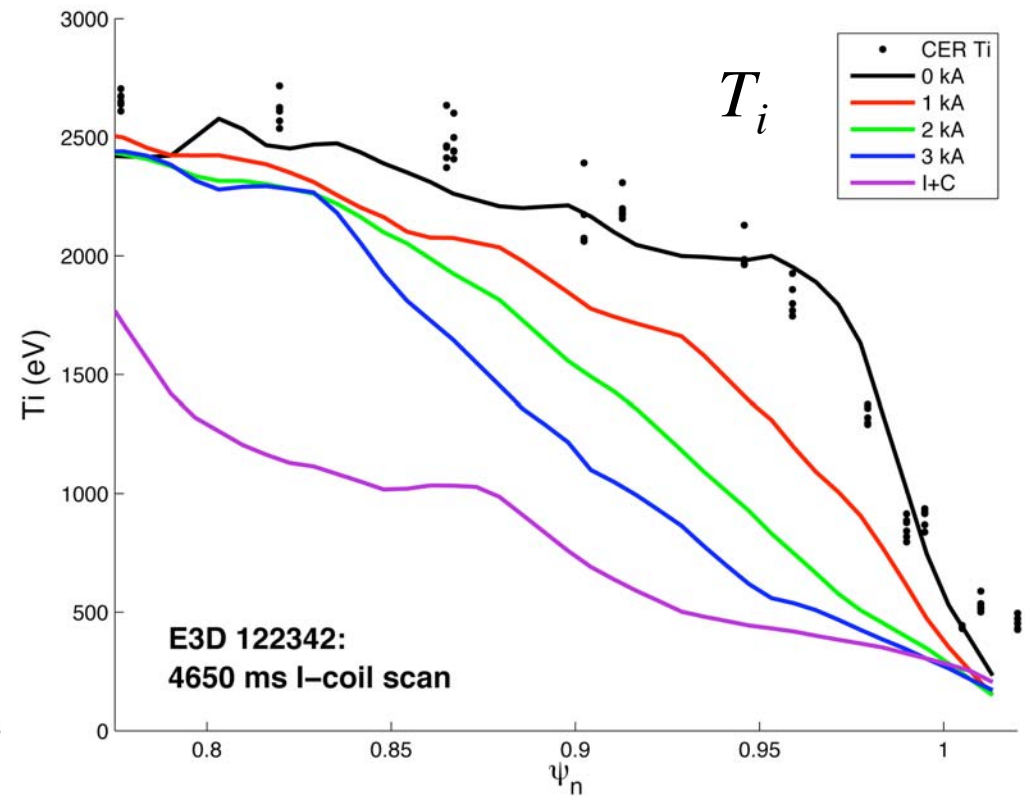
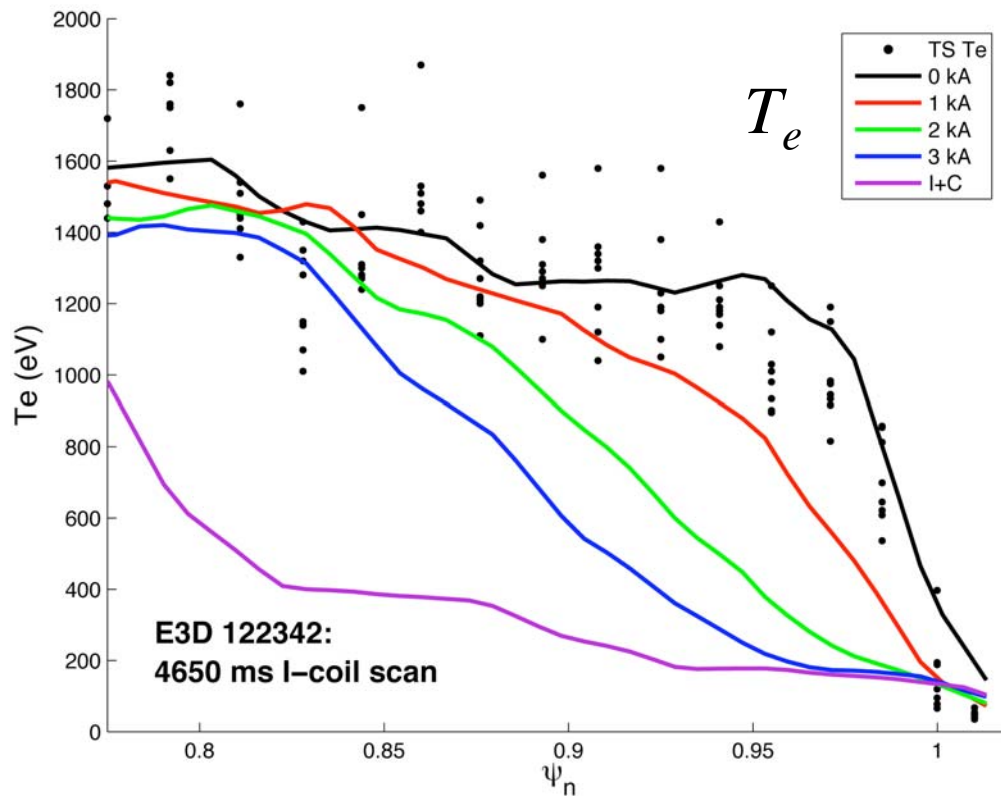
filtered D_α Xpt-TV:
123301 2170 ms



- Divertor strike pattern can be used to validate field model

As I-coil \uparrow : edge temperature cools \downarrow

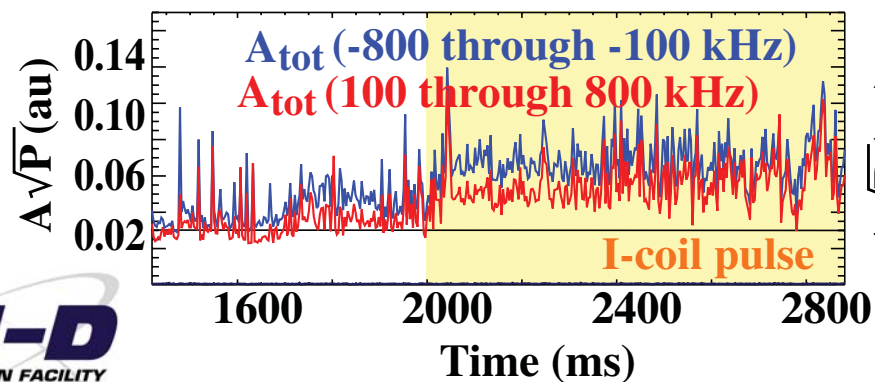
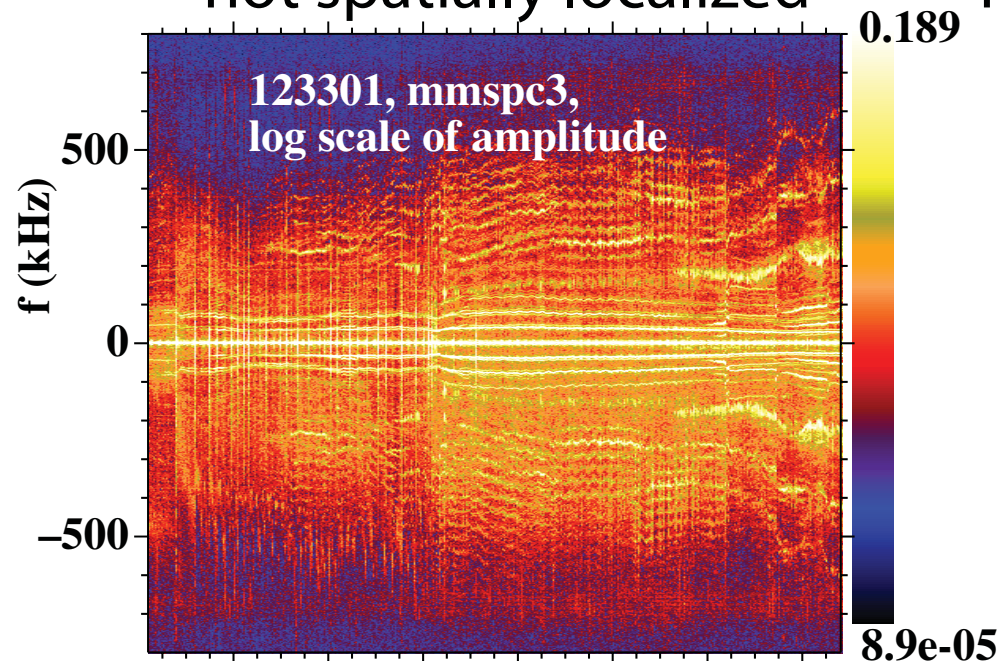
122342 at 4650 ms BC's: $T_e = 1.6 \text{ keV}$, $T_i = 2.6 \text{ keV}$ at $\psi_n = 77\%$



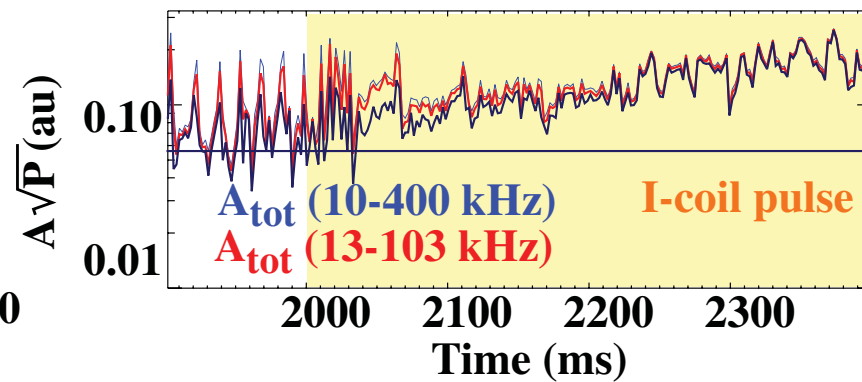
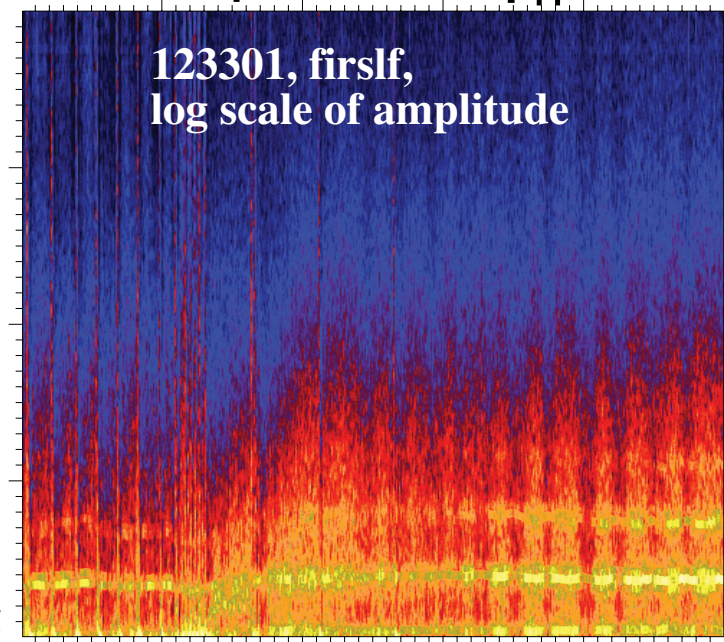
- Constant temperature BC's
- Edge stochastic layer cools relative to pedestal
 - remains hot compared to SOL

RMP application increases density fluctuations overall, including pedestal broadband turbulence

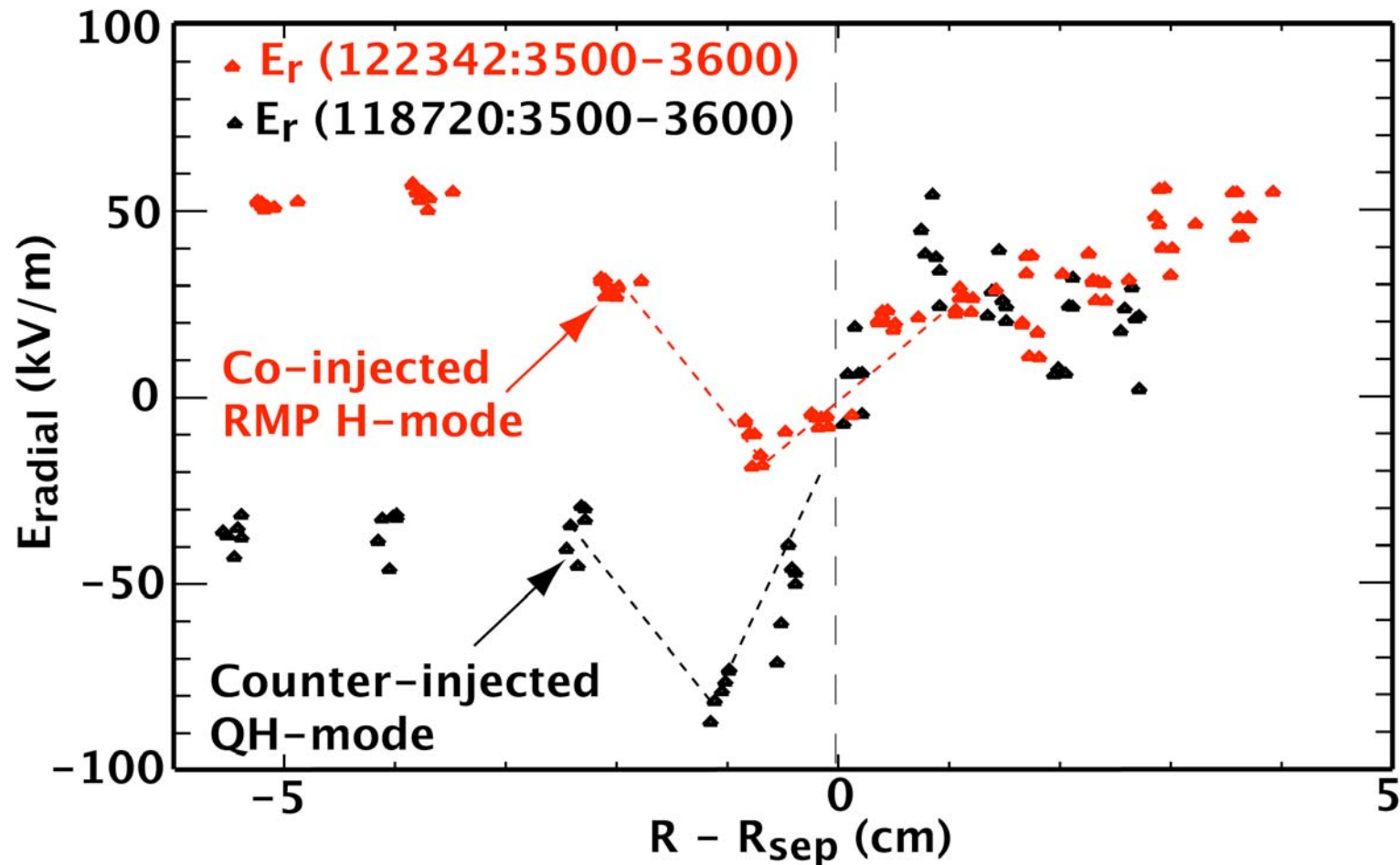
$k_\theta = 1 \pm 1 \text{ cm}^{-1}$ FIR scattering
not spatially localized



homodyne reflectometry
H-mode pedestal $\psi_n = 0.98$



RMP-assisted ELM-free H-modes have shallower E_r wells than QH-modes

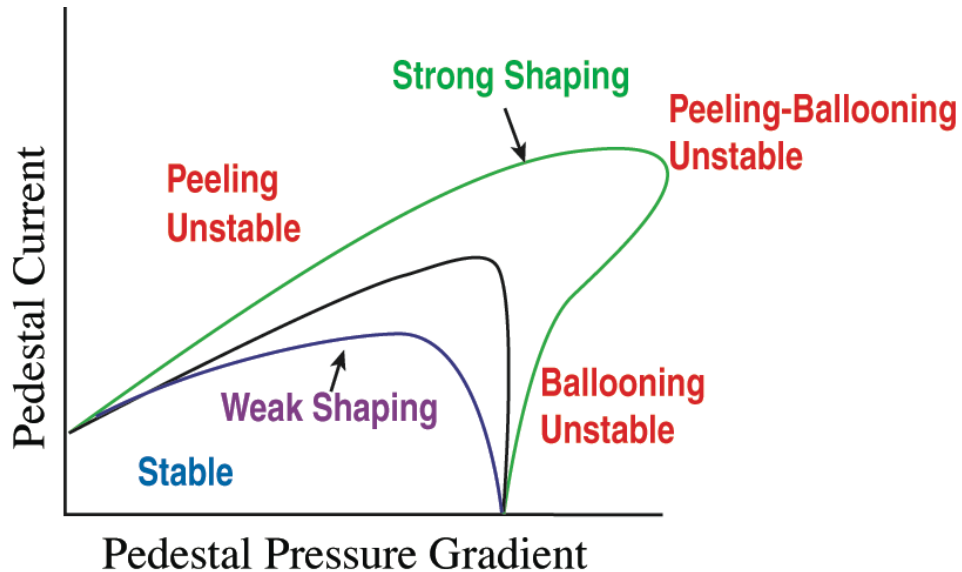


- E_r positive out to wall in both ELM-free plasmas; plasma potential \rightarrow 1 kV at wall.
- E_r shear near separatrix higher in QH modes.

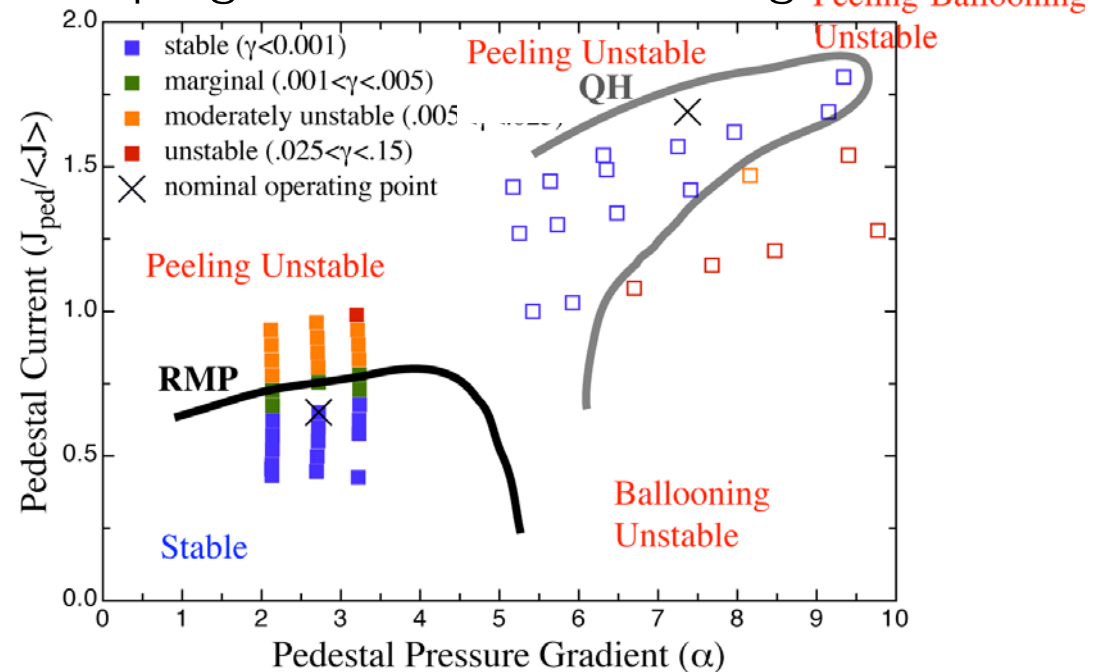
RMP ELM-free H-modes and QH modes both stable and near peeling boundary

Schematic P-B Stability Diagram

[P.B. Snyder, H.R. Wilson PoP2002]



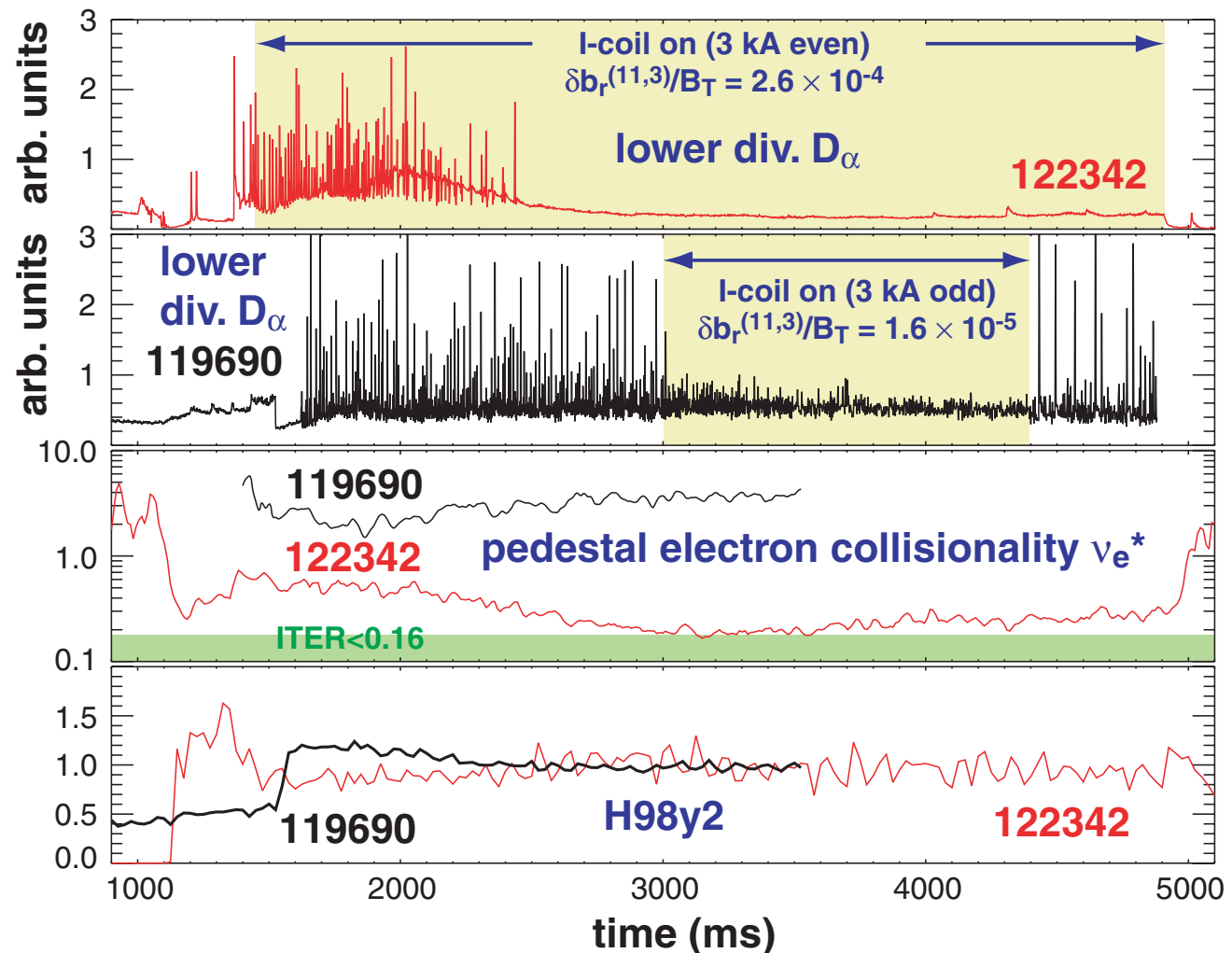
Shaping: RMP weak, QH strong



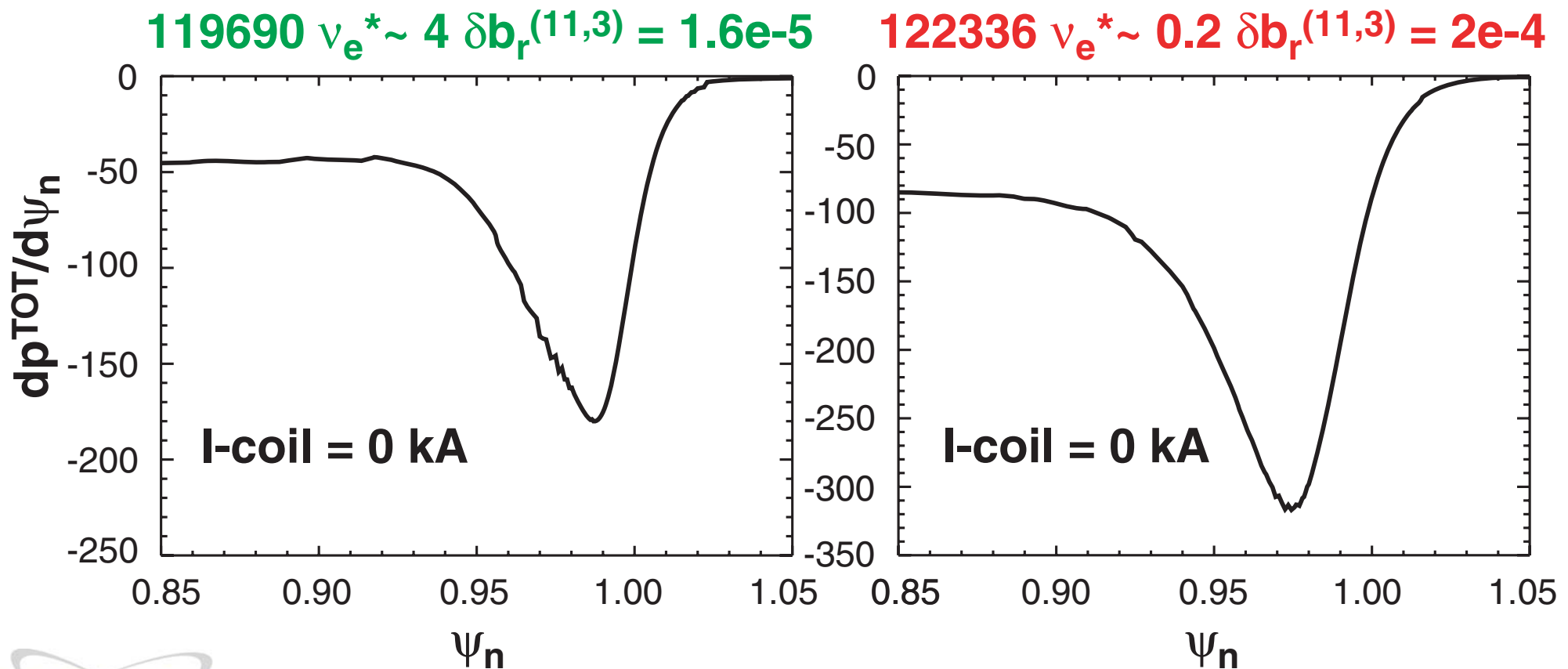
- **Strong shaping allows access to higher ∇P such as in QH-modes**
- **P-B stability boundaries are a strong function of plasma shape**
 - At present RMP ELM-free discharges can not access low ν_{e^*} in strongly shaped plasmas (because of pump location)
- **In 2006, low ν_{e^*} RMP ELM-free operations in strongly shaped plasmas will be investigated**

Edge Resonant Magnetic Perturbations (RMPs) have been used to eliminate large ELMs in DIII-D

- Large ELMs can be eliminated by reducing ∇P below the peeling-ballooning limit
P.B. Snyder, *next* contrib.
oral BO3.00009
- Large ELMs can also be suppressed in discharges where ∇P is essentially unchanged
 - Large ELMs are replaced by smaller, more continuous events (Type II ELMs?)

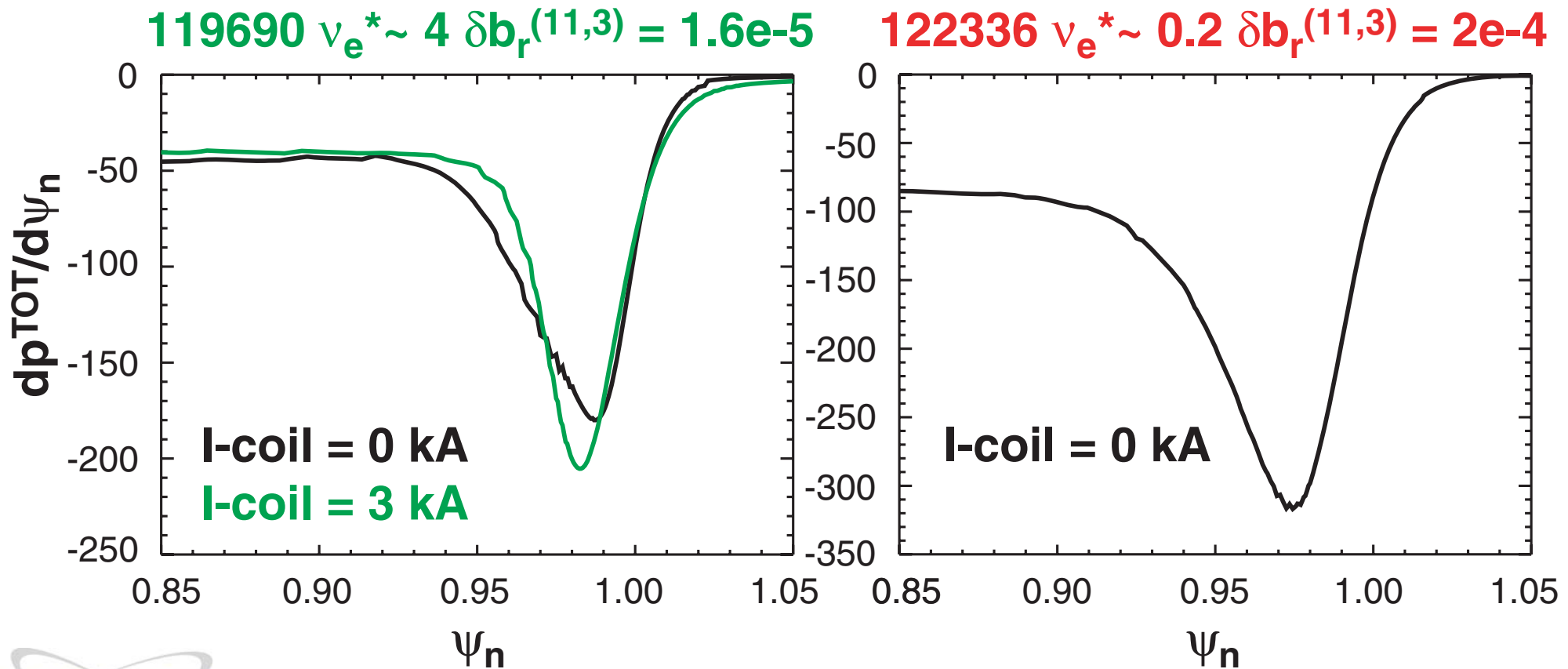


Edge RMP suppresses large ELMs without always significantly lowering ∇p^{TOT} .



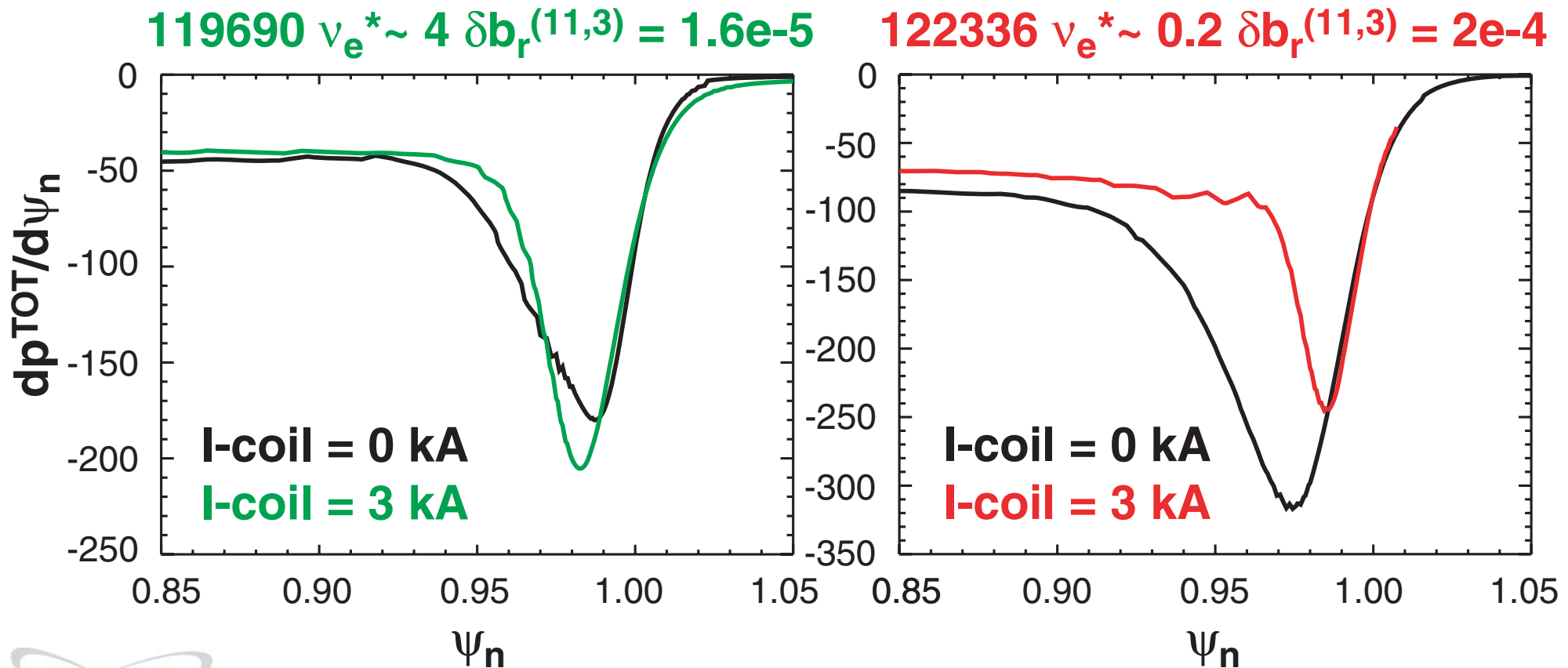
Edge RMP suppresses large ELMs without always significantly lowering ∇p^{TOT} .

- Small changes to $\nabla p^{\text{TOT}} \rightarrow$ always within error bar of peeling-ballooning bndry.



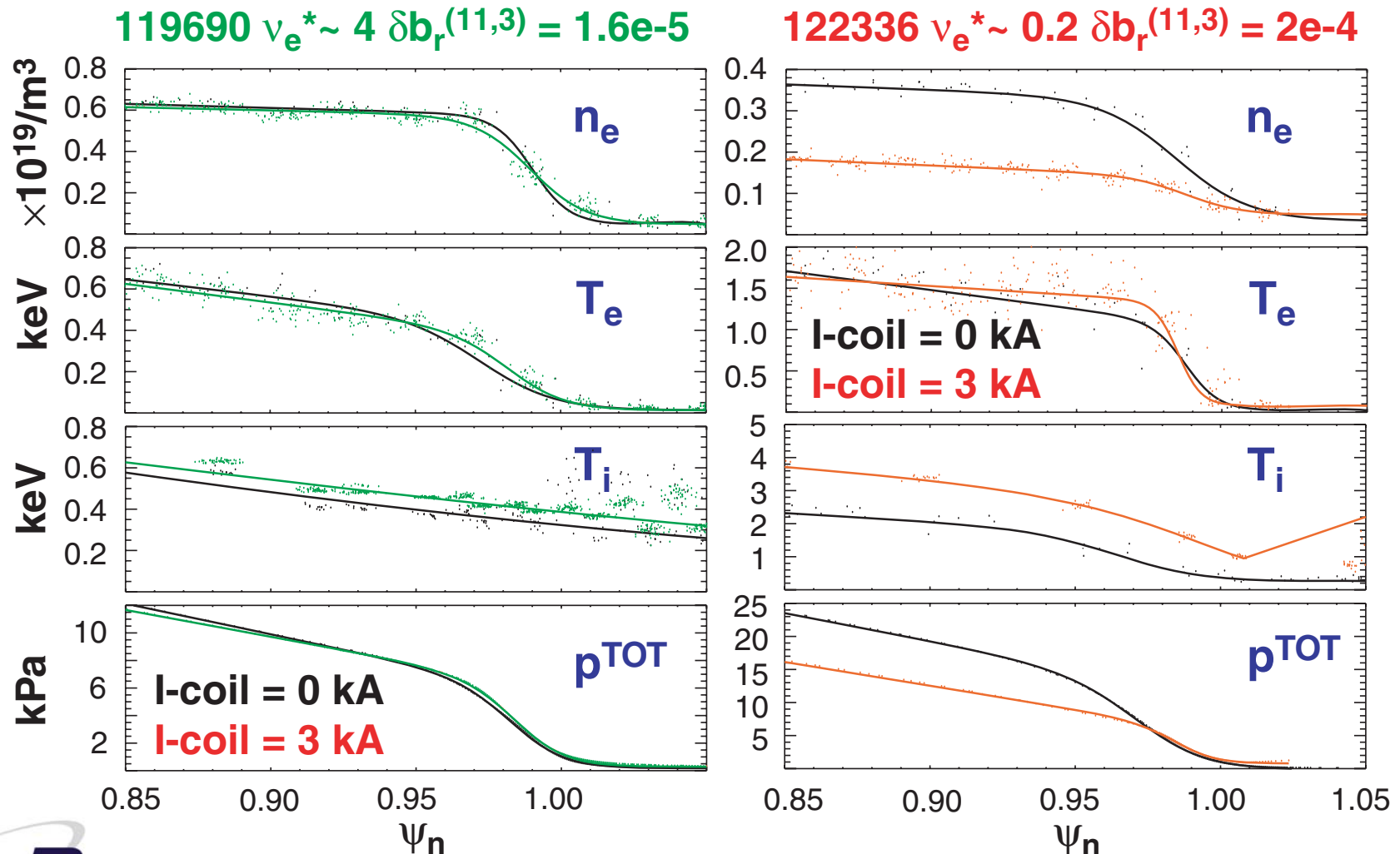
Edge RMP suppresses large ELMs without always significantly lowering ∇p^{TOT} .

- Small changes to ∇p^{TOT} → always within error bar of peeling-ballooning bndry.
- I-coil changes ∇p^{TOT} peak, width, & location → alters stability as planned.



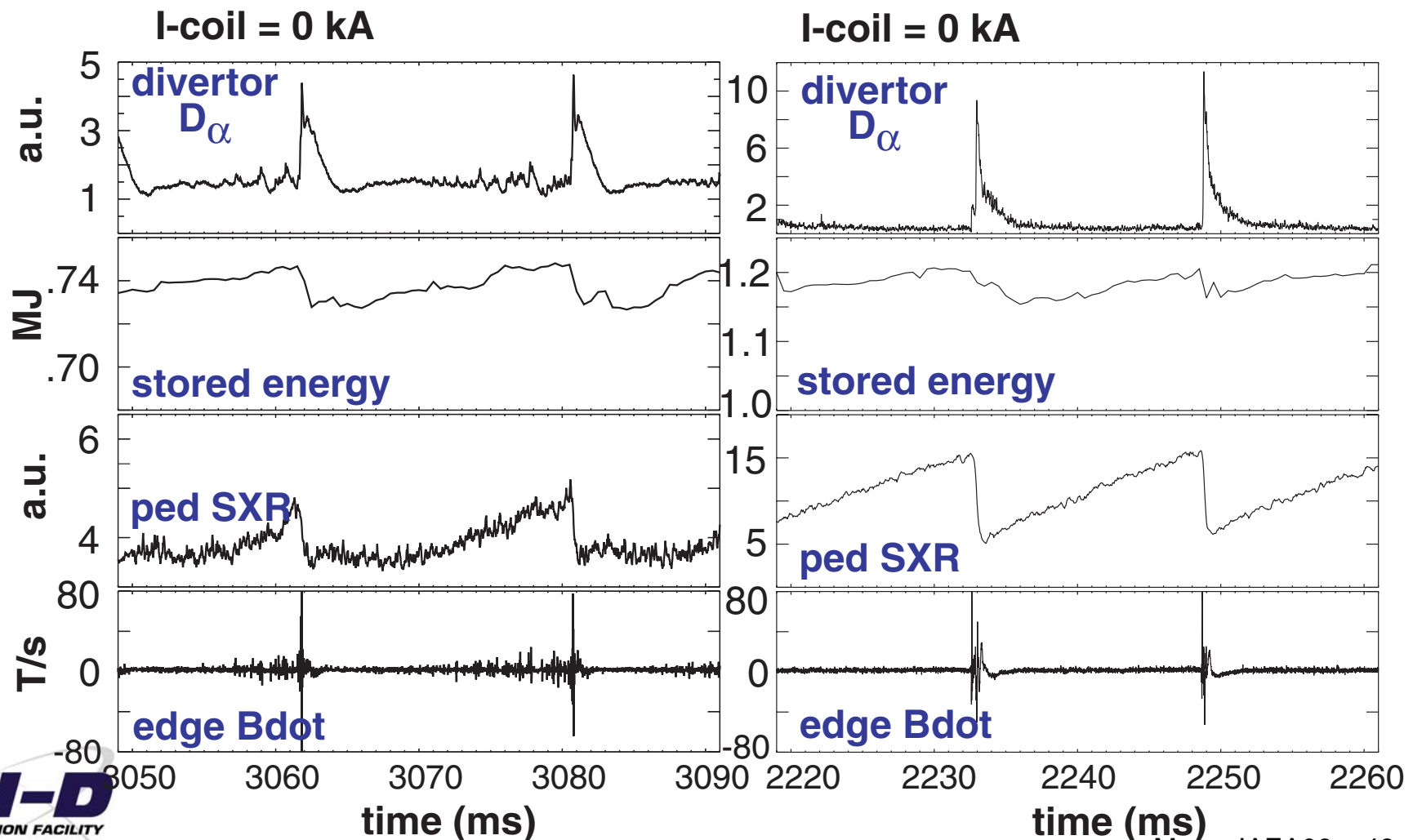
I-coil RMP has largest effect on density profile, not T_e profile.

- Not consistent with stochastic layer transport models .



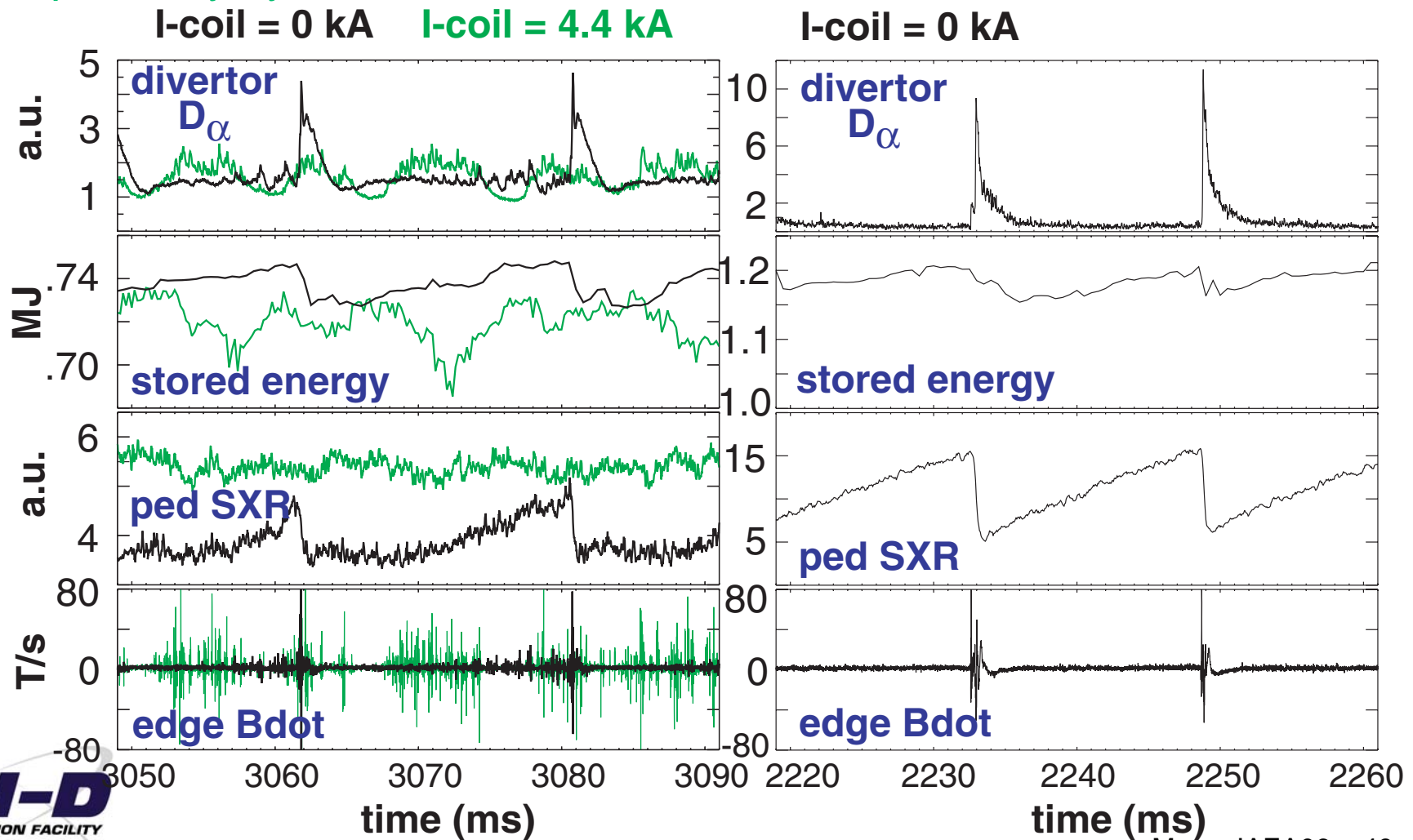
- Pedestal pressure decreases with increasing I-coil current

Pedestal thermal energy loss is correlated with bursts of magnetic fluctuations.



Pedestal thermal energy loss is correlated with bursts of magnetic fluctuations.

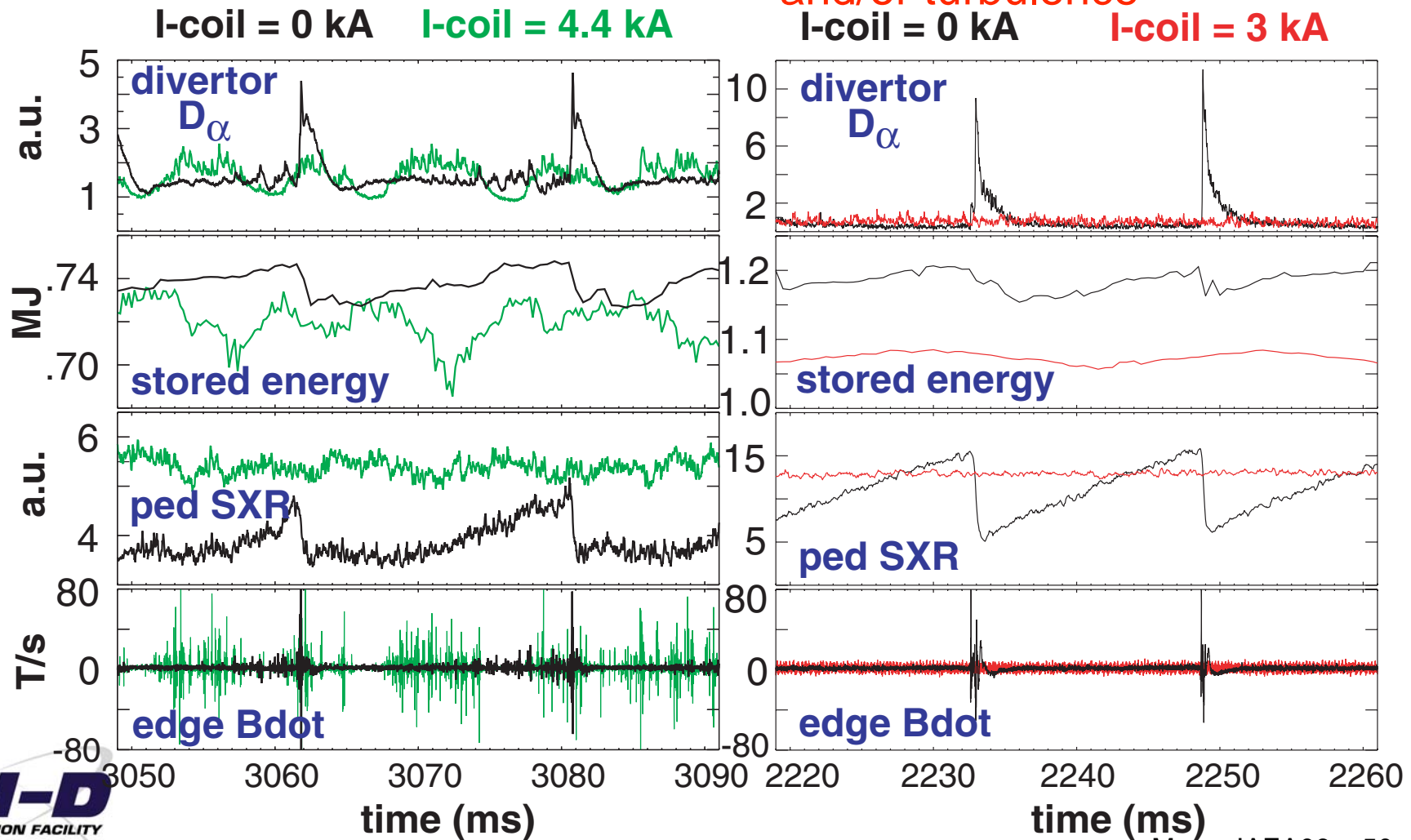
- At $v_e^* \sim 4$, enhanced small events
→ MHD mode →
transport duty cycle increases



Pedestal thermal energy loss is correlated with bursts of magnetic fluctuations.

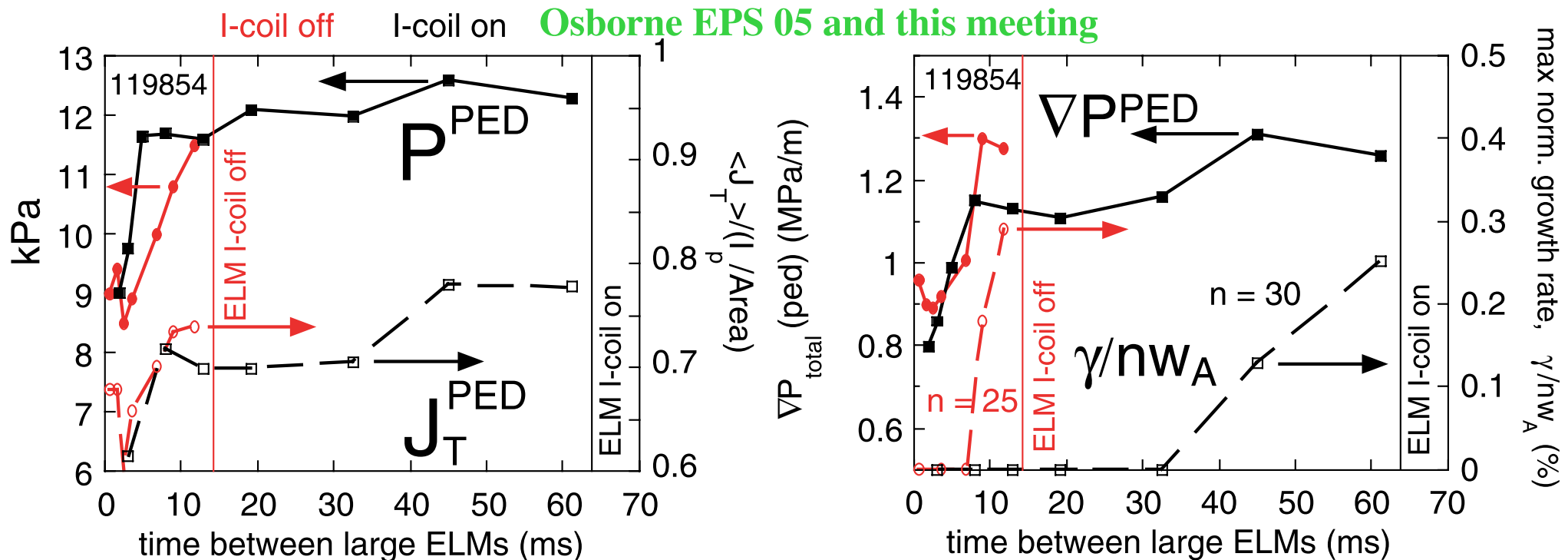
- At $v_e^* \sim 4$, enhanced small events
→ MHD mode →
transport duty cycle increases

- At $v_e^* \sim 0.2$, no small events ∅
quiescent → stochastic transport
and/or turbulence



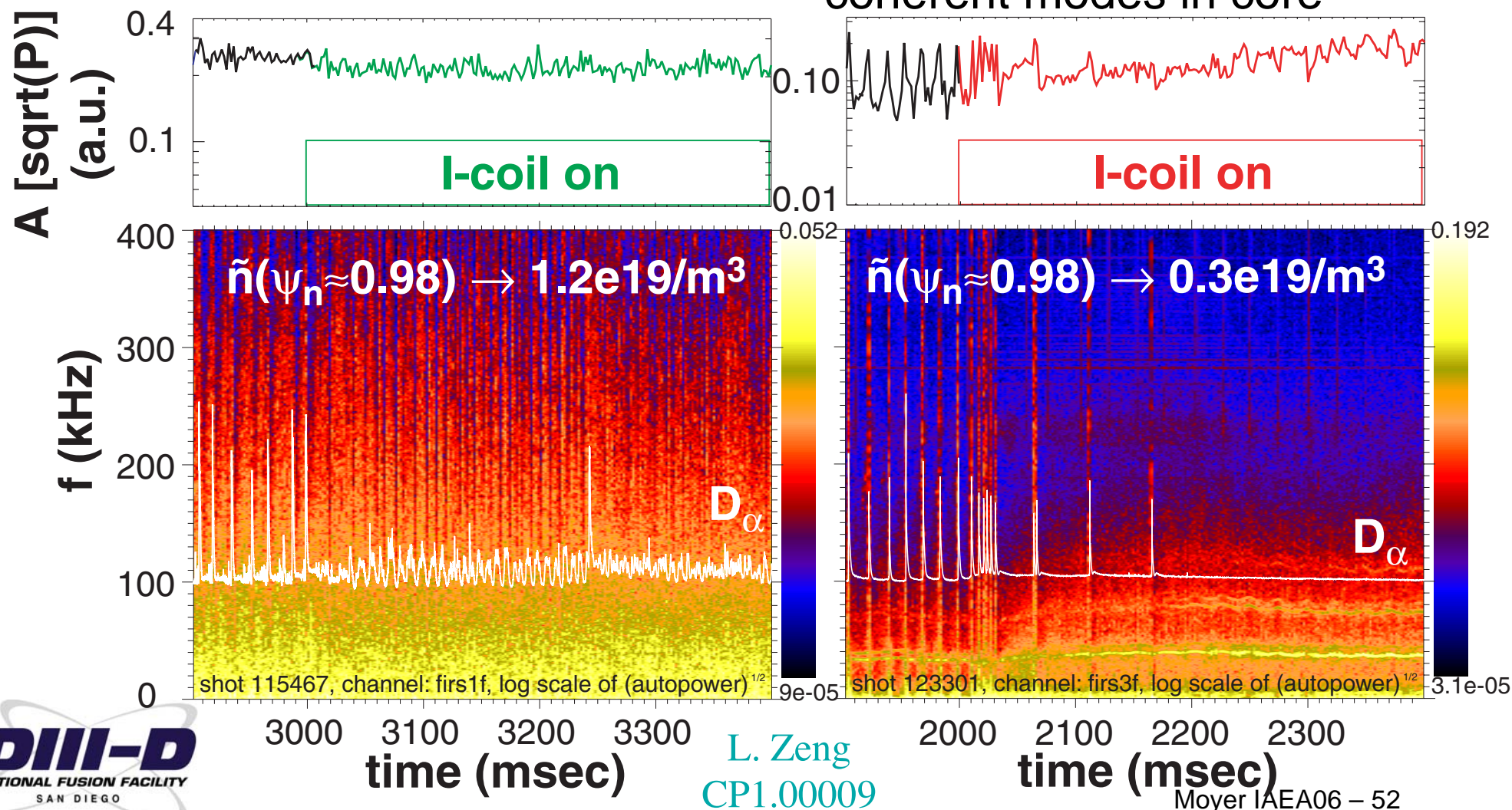
Recovery of pedestal ∇P to marginal stability slowed by small events during I-coil perturbation.

- Pedestal pressure P^{PED} & current J_T^{PED} similar after Type I ELM
- P^{PED} & J_T^{PED} > before Type I ELM with I-coil.
- Pedestal width > with I-coil
- Pedestal pressure gradient ∇P^{PED} recovers to marginally stable level more slowly
14 ms (I-coil off) → 64 ms (I-coil on)



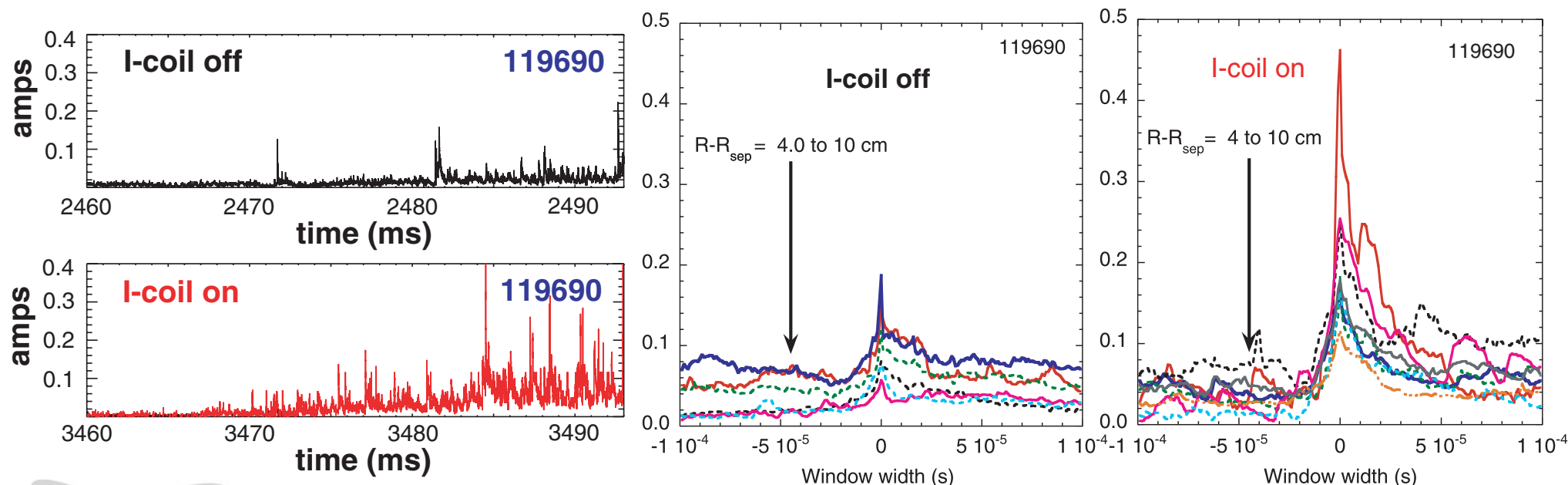
Density fluctuations in the pedestal change.

- At $\nu_e^* \approx 4$, $\tilde{n}_{rms} \sim$ constant, but more intermittency due to small ELM-like events
- At $\nu_e^* \approx 0.2$, \tilde{n}_{rms} increases as ELMs stop
- coherent modes in core



Intermittent transport during I-coil broadens the SOL and increases particle flux to wall

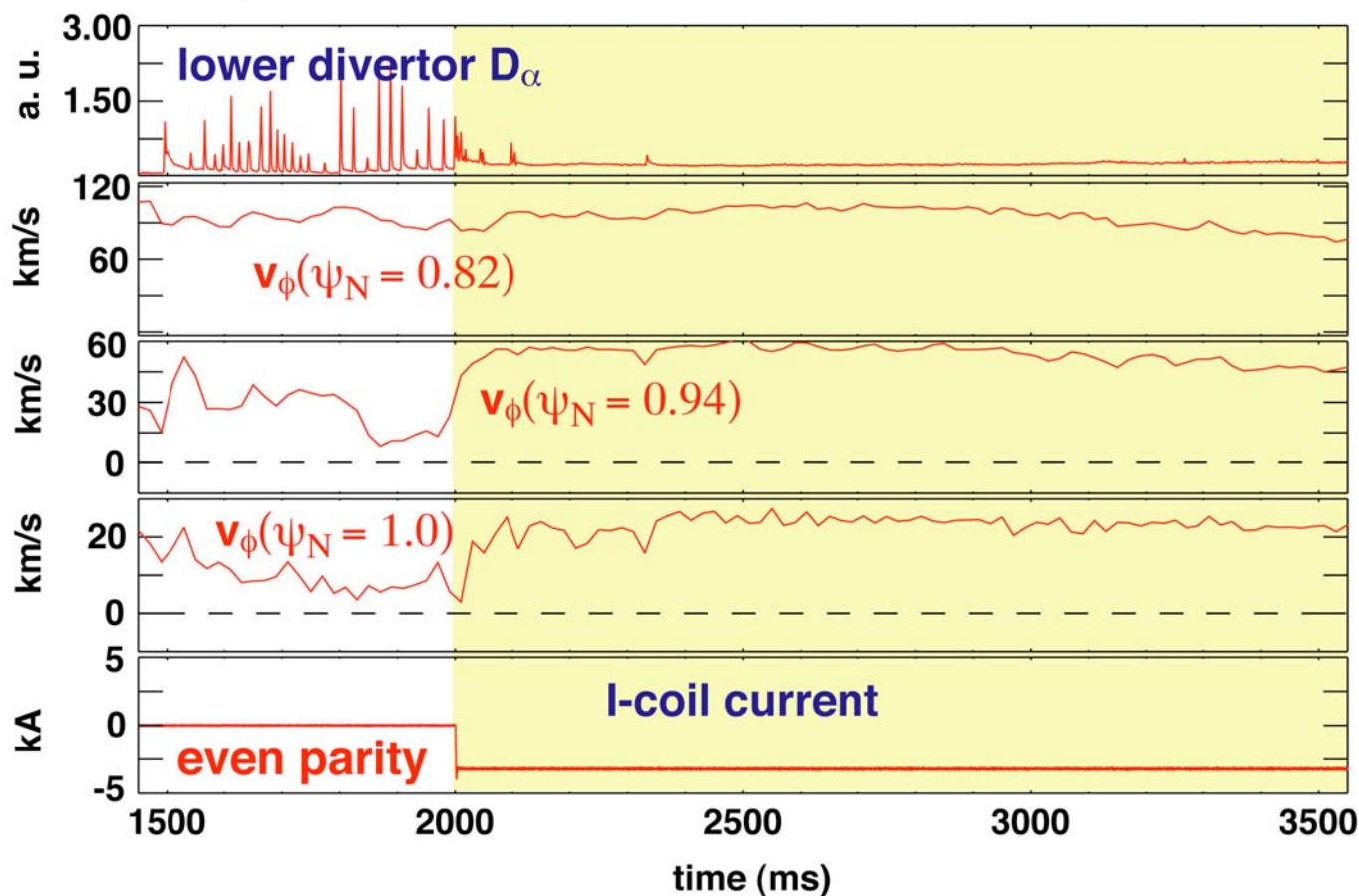
- Intermittent SOL transport increases during I-coil pulse.
 - For $v_e^* \geq 1$, burst freq. increases 2 \times , amplitude increases 2–3 \times
 - radial particle flux increases 2–3 \times
 - Increased power and particle flux to main chamber wall instead of divertor.
- Reciprocating probe I_{sat} near outer midplane



Even parity I-coil: ELM-free H-modes at ITER-relevant ν_{e^*}

T. E. Evans, K. H. Burrell, M. E. Fenstermacher, *et al.*, Phys. Plasmas, in press.

even parity/low ν_{e^*} : 122490



- Low density
 $\nu_{e^*} \sim 0.1$
- Type-I ELMs vanish within resonant q_{95} -window
- Edge rotation increases after ELMs disappear

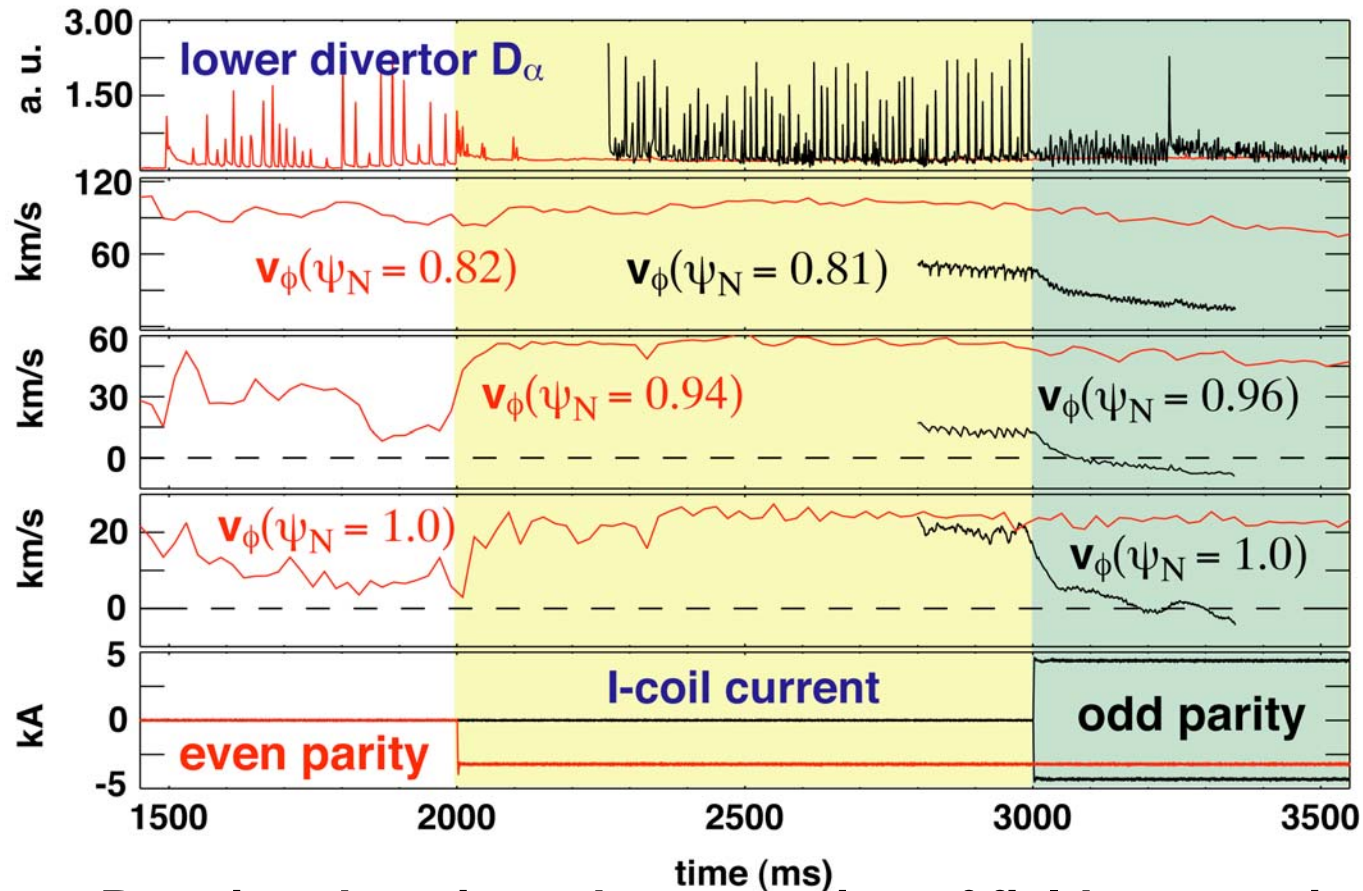
- Plasma maintains equilibrium for long times (unlike usual ELM-free)
- Steady-state transport must replace ELM transport

Odd parity I-coil: Type-I ELM-suppression

R. A. Moyer, T. E. Evans, T. H. Osborne, *et al.*, Phys. Plasmas 12 (2005) 056119.

even parity/low v_{e^*} : 122490

odd parity/high v_{e^*} : 115467



- Rotation damping taken as a sign of field penetration

- High density
 $v_{e^*} \sim 1$
- Type-I ELMs replaced with small Type-II grassy ELMS?
- Edge rotation decreases immediately after I-coil is energized